

Bone-Appétit! The influence of microorganisms on bone preservation in caves at Naracoorte, South Australia.

Thesis submitted in accordance with the requirements of the University of
Adelaide for an Honours Degree in Environmental Geoscience

Brooke Emily Lorincz

20th May 2020



THE UNIVERSITY
of ADELAIDE

**BONE-APPÉTIT! THE INFLUENCE OF MICROORGANISMS ON BONE
PRESERVATION IN CAVES AT NARACOORTE, SOUTH AUSTRALIA.**

BIOEROSION OF BONES IN CAVES AT NARACOORTE

ABSTRACT

The introduction of bacteria and fungi into subterranean environments are implicated as causal organisms for destruction of Palaeolithic art and vertebrate fossils. Taphonomy studies characterise modifications resulting from acidic and enzymatic exudates of microbial metabolisms, as fungal tunnelling, and bacterial pitting. However, few studies are privy to the natural biostratinomic history of the animal's decomposition, or the environmental variables and microbes influencing bone bioerosion. Hypotheses include early decomposition, soil burials, excessive nutrients and introduced diversity from tourism as catalysts of microbial erosion. By using modern in-situ bones from a decomposition study by Reed (2009) conducted within private caves in Naracoorte, South Australia, this study provided preliminary data on the associations between environment and the types of bioerosion that compromise bone preservation. Using Scanning Electron Microscopy (SEM) for characterising modifications, genetic profiling of microbial communities in caves and environmental cave assessments, this study observed diverse microbial communities are not conducive to bioerosion of vertebrate fossils in Naracoorte Caves. Moreover, the less diverse fungal communities within closed, oligotrophic caves appear to have greater degradative abilities during prolonged extraction of organic minerals.

Naracoorte Caves National Park captures the imaginations of the public and scientists for their invaluable retrospect on native faunal communities throughout the Pleistocene. Taphonomic analyses of the fossils recovered from NCNP are used toward research that enables investigation into ecological changes, geological histories, and faunal extinction by providing data models used in environmental research and management. Thus, taphonomic investigation of microbial destruction of vertebrate bone is a useful in understanding the diagenetic histories of important fossil assemblages.

KEYWORDS

Bone, fossil, bioerosion, taphonomy, Naracoorte Caves, microorganisms

TABLE OF CONTENTS

Abstract i

Keywords	i
List of Figures and Tables	8
1. INTRODUCTION	5
2. BACKGROUND	9
2.1. Geological and environmental setting.....	9
2.2. Study site and cave environment	11
2.3. Microbial metabolism.....	12
2.4. Taphonomic characterisation of bioerosion.....	13
3. METHODS	15
3.1. Bone and sediment sample collect.....	15
3.2. Faecal pellets and scapula.....	16
3.3. Atmospheric microbe sampling.....	16
3.4. Sample preparation and testing.....	18
3.4.1. Bone microscopy	18
3.4.2. Cave environment.....	18
3.4.3. Atmospheric gDNA profiling.....	19
3.4.4. Soil, bone and faecal pellet gDNA profiling.....	19
4. OBSERVATIONS AND RESULTS	20
4.1. Microscopy.....	20
4.2. gDNA profiling and microbial diversity.....	27
4.3. Cave environment assessment	36
4.3.1. Blanche Cave (BL-5U4,5,6).....	36
4.3.2. Victoria Fossil Cave (VF-5U1).....	36
4.3.3. Crawford's Dead Sheep Cave (CR-5U56).....	38
4.3.4. Lost Cave (LO-5U34)	40
4.3.5. Specimen Cave (SP-5U35).....	41
5. DISCUSSION	42
5.1. Bone taphonomy and microbes.....	42
5.2. Environment and microbes.....	46
6. CONCLUSIONS	50
7.Future Propects.....	53
8.Acknowledgements.....	53
Appendix A: Binary data for gDNA profiling.....	54
Appendix B: Microscopy.....	59

LIST OF FIGURES AND TABLES

Figure 1: a) Longview South Australia's south east. b) Locality of Naracoorte caves in south east region of South Australia. c) Geological identification of Naracoorte karst landscape and caves pertinent to the Kanawinka fault dividing the Eastern Naracoorte range (ESR) & western Naracoorte range (WNR). [Map c. adapted from Lewis 1976: South Australian CEGSA reference book].....13

Figure 2: Morphological representation of bone transection displaying characteristics of microbial erosion. 1) Type I Wedl tunnels 2) Type II Wedl tunnels 3) Lamellate MFD with hyper mineralised cuffing 4) Linear longitudinal MFD 5) Budded MFD. 6) Concentric cement lines of osteon lamellae. 7) Haversian canal. [Figure 6. adapted from Jans *et al.* 2008: Microbial bioerosion of bone].....18

Figure 3: a) LO-5U34 Experimental tibia deposited in 1998 by Reed (2009). Black square = sample area. b) Arrows point to corroded pits on area around nutrient foramen. c) Inside entrance of nutrient foramen. Square= organic growth with fine cracking on either side of growth. d) Area on cortical surface near nutrient foramen. Arrows indicate an increase of porosity around Volkmann's canals by formation of small bacterially induced corrosive pits and fine cracks. d) Magnification of pits from from (d) contains debris and vegetative bacterial infiltration of central fissure within pit. e) Distal end of tibia displays extensive corrosion and staining in (a) from sediment contact with low pH. f) Transect of cortical bone from distal shaft from (3) shows no characteristic bioerosion. Pitting along outer edge of cortical surface and widening of internal canals indicates environmentally influenced corrosion and elemental leaching of inorganic elements from the bone due to wet environments and soil pH.....27

Figure 4: a) CR-5U56 Experimental femur deposited in 1998 by Reed (2009). Black square= mid diaphysis with nutrient foramen and tuberosity. Evident staining from sediment and decomposition fluid. b) Surface shows widening and sediment infilling of pores. Corrosive paths from solubilisation of surface bone surrounds pores c) Fungal hyphae with sediment attachment protrudes from punched out pores. Degraded channels and fractures occur around hyphal extension. d) Transection of mid-diaphysis displays extensive infiltration within deltoid tuberosity. White square displays Wedl type I tunnelling from fungi, tunnels extend inward from the cortical layer of periosteal bone Haversian tunnels are filled with fungi and debris that has been brought in from adhering to the hyphae.....28

Figure 5: a) Scapula covered in fungal hypha from twilight area of CR-5U56. b) Fungal hypha protrude from cavity created within bone, c) Bundled hypha within cavity between periosteal bone and fibrous bone. d) Fungal hypha tunnel seen underneath to create sharp tunnel edges, suggesting new damage. Resorption pitting from osteoclast bone remodelling is around hypha. Debris adheres to hypha chitin layer suggesting sticky exudates.29

Figure 6: a) SP-5U35 Humerus with unknown deposition date collected from area around organic sediment cone. Slightly polished exterior. Sample square = middiaphysis with patina. b) Transection of mid-diaphysis directs arrows toward Haversian tunnel with visible branching hypha penetrating into surrounding osteon in Wedl II tunnels. c) Magnification of staining reveals site as potential phototropic attachment with fractures, porous bone exposed and clay-like deposits. d) Transection of same sample in (b) illustrates extensive bacterial infiltration characteristic of non-Wedl MFD, both linear-longitudinal (LL) and budded (BD).

No hypermineralisation is seen. The surface of the periossteal cortical layer of bone is beginning to sever from the bone from severe degradation.....30

Figure 7: Logarithmic scale of Fungal diversity from gDNA profiling of phyla at Naracoorte Caves. Samples collected from VF-5U1, CR-5U56, BL-5U4,5,6, LO-5U34.....31

Figure 8: Logarithmic scale of Bacterial diversity from gDNA profiling of phyla at Naracoorte Caves. Samples collected from VF-5U1, CR-5U56, BL-5U4,5,6, LO-5U34.....31

Table 1: Species list for gDNA profiling of fungi and bone and faeces samples from CR-5U56 and SP-5U35.....32

Table 2: Species diversity abundance for bacteria and fungi in gDNA samples from atmospheric samples in VF-5U1, BL-5U4,5,6; and soil and bone samples from LO-5U34 and CR-5U56.....34

Figure 9: VF-5U1 sample site map a) Atmospheric microbial settle plate sampling sites depicted on tourist map of Victoria Fossil Cave for bacteria and fungi in high disturbance (HD) and low disturbance (LD) areas. b) Site comparison for bacteria and fungi diversity c) Diversity comparisons between high disturbance and low disturbance zones.....35

Figure 10: a) Atmospheric microbial settle plate sampling sites depicted on tourist map of Blanche Cave for bacteria and fungi in high disturbance (HD) and low disturbance (LD) areas. b) Site comparison for bacteria and fungi diversity c) Diversity comparisons between high disturbance and low disturbance.....35

Figure 11: Linear regression analysis of total atmospheric microbes in VF-5U1 and BL-5U4,5,6 in sample order as distance from entrance. VF-5U1($R=0.04$) and BL-5U4,5,6 ($R=0.816909$).....36

Figure 12: Cluster analysis with Non-metric Multi-dimensional scaling (MDS) and Kulczynski group averages for dissimilarity testing. gDNA samples were given sample names by AGRF, they do not represent order from entrance, but represent each zone for VF-5U1 (Figure 9) and BL-5U4,5,6 (Figure 10). Caves show distinct communities of microbes. a) Distance representation for % of similarity between sites. b) Cluster analysis.....38

Figure 13: BL-5U4,5,6 a) Phototrophic microorganisms near light zone of entrance 5U4 create green film within porous limestone of cave structures. b) Slump of roof collapse funnels organic matter, water and directs airflow into main entrance chamber from entrance 5U4. c) Window 5U5, sediment cone displays nutrient and hydrological input sufficient to support plant growth within photic zone. d) Desiccated possum near entrance 5U4 caused by reduced microbial decomposition within an arid environment inducing mummification of soft tissue. Green phototrophic organisms grow around moisture of speleogenic drip in light zone..40

Figure 14: VF-5U1 a) Exposed fossil bed below viewing platform in main tourist chamber. The fossil bed displays numerous bones from the middle Pleistocene. b) Narrow renovated tourist path through limestone minimises air flow from connected chambers. Air flow is directed by visitor disturbance. c) Albert Edward grotto. Calcareous speleothems form by hydrological input from rainwater in soil. d) Surrounded by native landscape, a constructed entry point is sealed by a door to maintain security and within-cave environments. Cave is only illuminated by artificial lighting. [Victoria Fossil Cave. (2020). Images retrieved from <https://www.mountgambierpoint.com.au/attractions/victoria-fossil-cave>].....41

Figure 15: CR-5U56 a) Day 14 decomposition of Western grey kangaroo in humid rear chamber, experiment by Reed (2009) shows quick putrefaction b) Day 194 of decomposition skeleton and leaching of decomposition acids into soil (Reed 2009). c) Speleothems decorate the mid-section of the cave between the entrance and the rear chamber (Bourne 2020). d) Skeletal remnants of the Western grey kangaroo (Reed 2001) appear blackened from fluid staining (Bourne 2020).....42

Figure 16: LO-5U34 a) Day 14 decomposition of Western grey kangaroo in entrance chamber within twilight zone, experiment by Reed (2009). Bloat stage of decomposition and white hyphae of fungi is growing on legs. Sediment floor displays organic debris underneath kangaroo. b) Day 192 of decomposition skeleton. Skeleton has been disarticulated by consecutive pitfall victims trampling the kangaroo. Bone is covered in fungi (Reed 2009). c) The remaining bones have been scattered within the chamber, the tibia was collected for taphonomic identification. On distal end of tibia touching the sediment floor, algae are notable. d) Pelvic girdle of Western grey kangaroo and associated rocks are covered in green algae.....44

Figure 17: A conceptual flow diagram for observations and conclusions made within this study. Diagram details cave types, environments, factors affecting environments, the microbes associated and the effect on the fossil bone.....54

1. INTRODUCTION

Microbial modifications to bone, otherwise known as bioerosion, is portrayed as a common form of deterioration during skeletal decomposition (Fernández-Jalvo et al. 2010, Jans 2008, Hackett 1981) . Alterations to bone structure are created through metabolic excretions from bacteria, fungi, and cyanobacteria. These excretions solubilise organic and inorganic bone, forming various tunnels and re-mineralised pits throughout the cortical bone and on the periosteal surface (Hackett 1981, Janaway et al. 2009, Marchiafava et al. 1974, Wedl 1865). The dissolution of bone structure

compromises the mineral and structural integrity and becomes improbable that the bone will endure environmental challenges, such as burial and compaction, and will be destroyed prior to fossilisation (Fernández-Jalvo et al. 2010, Trueman and Martill 2002)

Mineralized hyphae found in long bones of Late Cretaceous dinosaurs (Owocki et al. 2016) and bioerosion displayed on Silurian and Pleistocene remains (Trueman and Martill 2002) demonstrates a long history of microorganisms involved in bioerosion (Owocki et al. 2016). Archaeological observations by Jans (2008) suggests bacterial pitting is common to human remains and fungal within animals. Although both characteristics are rarely a mutual occurrence, differences within the pre-burial environment determine the type of modifications (Jans 2008, Tibbett and Carter 2009). Variance in bioerosion provides taphonomic insight into pre-burial histories and provides information toward a cumulative understanding of the key environmental variables contributing toward microbial erosion, bone diagenesis and fossilization (Harke 2000, Pesquero and Fernandez-Jalvo 2014, Kendall et al. 2018).

Naracoorte Caves National Park (NCNP), is an invaluable time capsule for 500,000 years of Australia's natural faunal history (Reed 2012, Reed and Bourne 2000). The comprehensive assemblage of Quaternary vertebrate fossils discovered in diverse cave environments arbitrarily exhibit bones with microbial modifications throughout the stratigraphy (perscomm. Elizabeth Reed 2020); however, NCNP has no current research on relationships between the effect of cave environments on bioerosion of vertebrate fossils.

Between 1998 and 2001, Reed (2009) conducted a decomposition study within private caves at Naracoorte which provided discrete observations of microbial persistence on

kangaroo skeletons (Reed 2009). Consequently, the relatively undisturbed sites sustained the in-situ skeletons and together with a well-documented necrology offers opportunity for a modern assessment of microbial accumulations and bioerosion of bone within variable cave environments.

The overarching aim of this thesis is to provide insight into microbial degeneration of bones in caves at Naracoorte. This will be achieved by using site specific microbial profiling in tourist caves, Blanche Cave and Victoria Fossil Cave, and taphonomic evaluation of bioerosion of modern bones found in private caves.

The key hypotheses for this thesis are:

- Microbial activity during the decomposition of vertebrate remains in caves compromises the preservation of bone by modifying the bone surface and structure.
- Cave type, within-cave conditions and degree of disturbance influence the diversity and type of microorganisms that bones will be exposed to.

The following specific aims will be addressed:

1. Provide individual environmental assessments of sample caves (sediment pH, temperature, humidity/hydrology, and structural description) using current evaluations and published data.

2. Obtain atmospheric microbial profiles within caves using gravity settle-plate techniques to determine taxonomic diversity of high and low disturbance areas within disparate tourist caves.
3. Distinguish microbial diversity within sediment samples from two caves where previous decomposition studies have been conducted (Reed 2009) and contrast to species pervasions of modern bone samples in contact with sediment.
4. Prepare and analyse all microbial assessments of cave samples submitted for genetic profiling as per Australian Genome Research Facility (AGRF) for Next generation sequencing (NGS) using 16SRNA and 18-ITS targets to delineate bacterial and fungal species.
5. Provide insight into notable relationships between microbial diversity and cave environments using nonmetric multidimensional scaling and morphological analyses of taxa.
6. Identify taphonomic signatures of microbial activity on cortical surfaces and cross sections of modern bones through palaeohistological preparation and scanning electron microscopical (SEM) imagery using backscattered electrons (BSE).
7. Contrast Naracoorte cave environments with taphonomic evaluation of bones to determine cave environments most conducive to higher degrees of bioerosion.

1. BACKGROUND

1.1. GEOLOGICAL AND ENVIRONMENTAL SETTING

Naracoorte Caves National Park (NCNP) is in the south east region of South Australia, around 100 km from the coast (Figure 1). Cave development at Naracoorte occurs primarily within an uplifted portion of the Gambier Limestone along the Naracoorte East Range (White and Webb 2015, Bourman et al. 2016). This limestone was deposited by shallow inland seas during the late Eocene to early Miocene and is overlain by Pleistocene calcarenite dunes, created by marine transgressions and regressions (Bourman et al. 2016, White and Webb 2015). Phreatic solution of the limestone in the early Pleistocene formed the karst structures seen at NCNP (Bourman et al. 2016, Reed and Bourne 2000). First discovered by Reverend Tenison-Woods (Reed 2012) a replete assemblage of Quaternary vertebrate fossils is found within the caves spanning the last ~500,000 years (Macken et al. 2011).

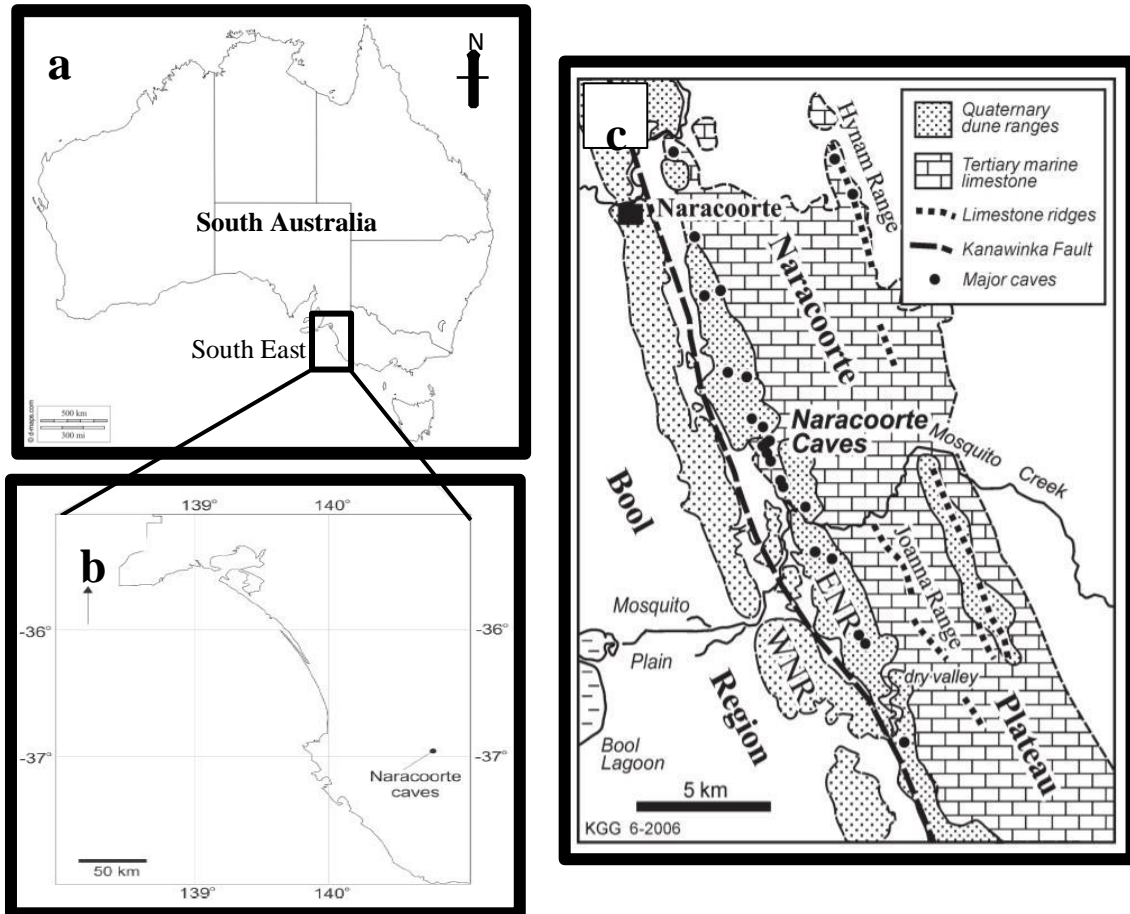


Figure 1: a) Longview South Australia's south east. b) Locality of Naracoorte caves in south east region of South Australia. c) Geological identification of Naracoorte karst landscape and caves pertinent to the Kanawinka fault dividing the Eastern Naracoorte range (ENR) & western Naracoorte range (WNR). [Map c. adapted from Lewis 1976: South Australian CEGSA reference book].

2.2. STUDY SITE & CAVE ENVIRONMENTS

Five caves at Naracoorte were chosen for sampling. Blanche Cave (BL-5U4,5,6) and Victoria Fossil Cave (VF-5U1) occur within the NCNP and are both show caves for tourists. These caves were sampled for atmospheric microbial profiles. Two caves on private land and another cave in adjacent scrubland were chosen for soil sampling and bone sampling. These caves were Specimen Cave, (SP-5U35) Crawford's Dead Sheep Cave (CR-5U56) and Lost Cave (LO-5U35). The latter two caves were chosen as were experimental sites for a decomposition study by Reed (2009) and contained bones of known age. All caves at Naracoorte are registered under the Australian Karst Index and given a unique reference number such as 5U1, consisting of '5' for South Australia, 'U' for Upper South East Region and a numerical value for the cave entrance.

NCNP is in native scrubland with partially cultivated grounds for tourism, approximately 12 kms south of Naracoorte township. Surrounding properties are managed by Forestry SA or privately owned and used for agriculture and viticulture. Typical caves at Naracoorte are large roof collapse or solutional chambers joined by passage systems created by phreatic solution (White and Webb 2015). Hydrology within the systems is generally limited to input from entrances following rainfall, vadose flow through the limestone or input from ground water. Shelter from seasonal fluctuations on the land surface provides stable subterranean conditions and limits weathering of exposed vertebrate fossils on the cave floor (Behrensmeyer 1978). The shape and size of cave entrances determine the within-cave environmental conditions such as: light, temperature, soil pH, hydrology, airflow, humidity, deposition, and dispersal of allochthonous materials. All these factors potentially influence the occurrence and taxonomic composition of microbial communities within caves.

2.3 MICROBIAL METABOLISMS

Microorganisms (Fungi, bacteria, yeast, archaea) use catabolic metabolisms, decomposition of larger molecules into smaller units, for cellular energy (Brehm et al. 2005, Metcalf et al. 2016, Pritsch and Garbaye 2011). Secretion of digestive enzymes and acids into their surroundings solubilise their substrate. Broad classifications of microbes are; aerobes (require oxygen) and anaerobes (Oxygen is toxic and depend on other matter as electron receptors). From a nutritional perspective, three main physiologic types of microbe exist: the heterotrophs (chemoorganotrophs), which effectively decompose organic matter (carbohydrates, lipids, and proteins). The autotrophs (chemolithotrophs), preferring inorganic matter (Ammonia, Sulphur, calcium, phosphorous) enabling persistence in low-nutrient, oligotrophic conditions. And, photosynthetic bacteria (phototrophs), which contain pigment cells and convert sunlight into chemical energy, using weak acids to solubilise their substrate in which to anchor themselves (Gadd 2011, Kasem et al. 2011, Metcalf et al. 2016, Ogórek et al. 2016, Paczkowski and Schütz 2011)

Taphonomy studies by Márquez-Grant et al. (2017) discovered temporal changes over 4 years of decaying bone. Collagenase producing bacteria (Firmicutes and Bacteroidetes) decreased, as environmental bacteria (Actinobacteria, Alpha and Gamma proteobacteria) increased. Bacteria has dominated bioerosion of archaeological bones; however, Jans (2008) observed animal bone was most likely to display fungal infiltration, through removal of flesh and dismemberment of scavenging which prevented dispersal of endogenous bacteria into extremities.) (Jans 2008, Jans et al. 2004). Hackett (1981) suggested bacterial erosion occurs during early putrefaction from endogenous anaerobes from the intestines invading surrounding tissues and vessels.

Meanwhile, Jans (2004) proposes environmental variables inhibiting initial bacterial MFD can later occur from soil microbes and environmental influences.

Although, apart from bacterial and fungal symbioses seen in lichen on surfaces of Cenozoic bones (Hospitaleche et al. 2011), it is rare to have both fungal and bacterial erosion within the same bone (Jans et al 2004). This may be due to competitive exclusion or in response to micro and macroenvironmental changes in temperature, moisture, available nutrition, and UV radiation, with success of microbial growth contingent to the realised niche (Behrensmeyer 1978, Jans 2008, Paczkowski and Schütz 2011)

2.4. TAPHONOMIC CHARACTERISATION OF BIOEROSION

In 1865, Wedl described two main types of fungal bioerosion discovered from a rib bone extracted from a well. Type I, occurring often as single tunnel, or branched, boring inward from the periosteal margins and is 10–15 μm in diameter (Figure 2) (Hackett 1981, Wedl 1865). And, Type II, 4-8 μm in width, ~0.25 mm below the cortical surface which extend out from the point of entry, usually from within an osteon, in branching networks of tunnels. Both types of tunnels appear unobstructed by cement lines of the concentric lamellae around the osteon (Figure 2) (Hackett 1981, Wedl 1865).

Marchiafava (1974) corroborated this through applying *Mucor* fungi to autoclaved human bone. Activity was associated with the calcified bone, noticing ‘saucer-like’ surface notching and ‘punched out’ holes where the fungal hyphae penetrated the surface (Marchiafava et al. 1974). Surface tunnels displayed sharp edges in contact with the flattened hyphae on surface bone, with no decalcification of bone, ascribed to removal of both organic and inorganic bone simultaneously (Fernández-Jalvo et al. 2010, Marchiafava et al. 1974). Whereas, decalcification and roughened tunnels

occurred around hyphae appearing in an aged form of degeneration. Due to lack of redeposited minerals of internal tunnels, Marchiafava suggested fungi excreted enzymes and acids (experiments assigned citric acid to *Mucor*) to solubilise and resorb the substrate during apical extension of hyphal growth (Fernandez-Jalvo 2016, Jans 2008, Kendall et al. 2018, Marchiafava et al. 1974)

Wedl (1865) ascribed all destructive foci as fungi, although the appearance of ‘cuffing’ from mineral redeposition was rejected as typical of fungi by Marchiafava (1974), Hackett (1981) defined this distinctive trait as bacterial microscopical focal destruction (MFD). Hackett (1981) described visible expansion of corrosive foci around the osteons and within cortical bone as non-Wedl characteristics. Patterns range between budded, lamellate, and linear-longitudinal with mineral redeposition around the MFD site.

Multiple studies by Hospitaleche (2011), Fernandez-Jalvo (2016) and Popović et al. (2015) described damage from phototrophic bacteria and lichen. Infiltration of water-holding pores on the bones surface, penetrate deeper bone layers and used as a holdfast (Hospitaleche et al. 2011, Popovic et al. 2015) .The acid leaches under the periosteal layer and causes extensive surface cracking, flaking, and sloughing of entire layers of bone. There is notable formation of secondary clay minerals and formation of a patina or crystalline surface at point of attachment (Popovic et al. 2015)

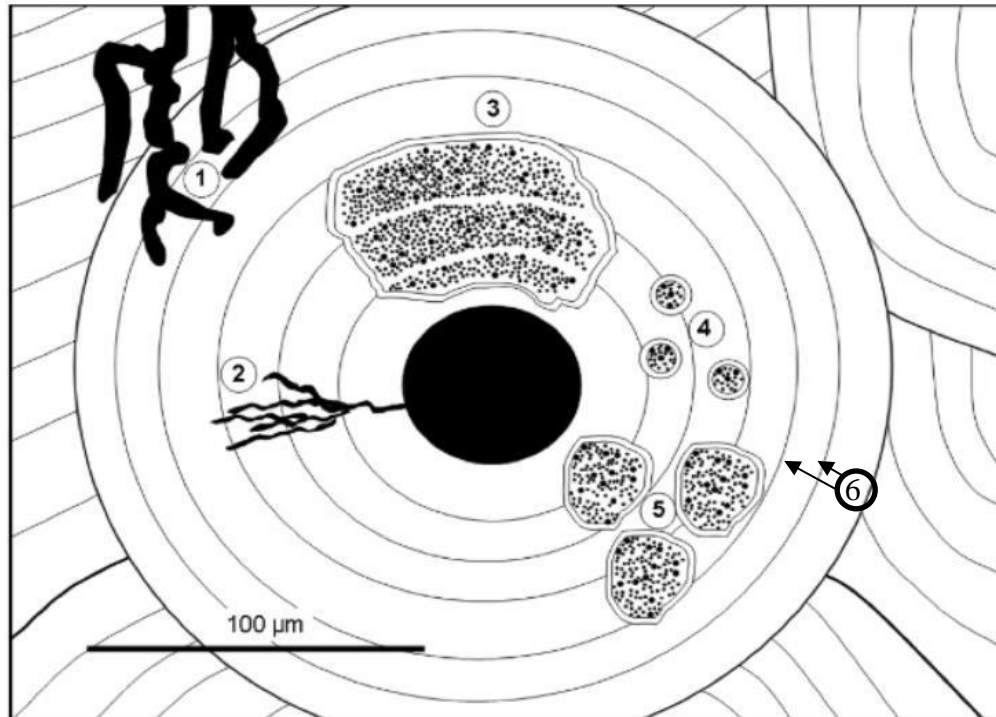


Figure 2: Morphological representation of bone transection displaying characteristics of microbial erosion. 1) Type I Wedl tunnels 2) Type II Wedl tunnels 3) Lamellate MFD with hyper mineralised cuffing 4) Linear longitudinal MFD 5) Budded MFD. 6) Concentric cement lines of osteon lamellae. 7) Haversian canal. [Figure 6. adapted from Jans *et al.* 2008: Microbial bioerosion of bone].

3.METHODS

3.1. BONE AND SEDIMENT SAMPLE COLLECTION

To test the hypothesis that microbial activity modifies bone surfaces during decomposition of vertebrate carcasses, 20 bone samples were collected from surface sediments of 3 caves for microscopic characterisation of surface modifications. Six bones, including 3 experimentally placed bones in sites LO-5U34, CR-5U56 by Reed (2009) in 1998 known to have had fungal growth were sampled as well as other modified specimens, including samples from SP-5U35. One scapula near the entrance of CR-5U56 displayed heavy fungal presence.

Bones collected from the twilight zone of LO-5U34 had conspicuous algal growth within the immediate depositional area. A tibia with the least phototrophic growth was

chosen and areas of growth perpetuated after collection were bleached in 1:3 of 4% hypochlorite and water back in the laboratory, though growth continued within other regions of the bone. Bones from CR- 5U56 were collected from the rear chamber and SP-5U35 at varying distances to the light zone and within the moist, organic deposits of the sediment cone. Bone samples were sealed in zip lock bags to minimise further exposure to airborne microbes and transported in a light-proof container to limit growth of phototrophic species. Some bone samples were later sub-sampled for microbial profiling.

Sediment from decomposition sites in CR-5U56 and LO-5U34 were collected into a zip lock bag from the top 3 cm of the cave floor for biomolecular profiling.

A further 3 three soil samples were collected from CR-5U56 and SP-5U35 for Environmental pH testing. Fire safety restrictions prevented further access to LO-5U34 and only one soil sample was available to represent pH.

3.2. FAECAL PELLETS AND SCAPULA

Possum faecal samples from SP-5U35, a fox faecal sample and sheep scapula from CR5U56 were collected by Liz Reed and Steve Bourne for significant presence of fungal growth (Table 1) All samples were collected into ziplocked bags and 50 ml containers and kept at <15°C during transport.

3.3. ATMOSPHERIC MICROBE SAMPLING

To test the hypothesis that cave type, environmental conditions and disturbance influences the diversity and type of microorganisms bones will be exposed to, atmospheric microbial profiling samples were collected at various points within the

tourist caves BL-4,5,6 and VF-5U1 for biomolecular profiling to determine microbial community composition.

Koch sedimentation is a passive gravity method for collecting aerosolizing microbes onto nutrient plates (Jiang et al. 2017, Zhang et al. 2017). Manufactured nutrient plates were selected for pH ranges; Malt extract (pH 3.6), Potato Dextrose (5.6), Czapek Dox (7.3) and Brain Heart Infusion (7.4). In sample sets of 4 plates, 10 zones in VF-5U1 (Figure 8) and 6 zones in BL-5U4,5,6 (Figure 9) were selected along corridors, paths and within chambers corresponding to tourist disturbance and low tourist disturbance. Sample sets were positioned prior to a directed cave tour and collected after 1.5 hours to allow microbial sedimentation (17min/m) to occur from disturbance of tourists and natural convection. For controls of microbial diversity, a set of plates was positioned within 3 m from both cave entrances on the exterior surface.

The plate lids were sealed in-situ with parafilm to minimise contamination. Samples were refrigerated at $\sim 7^{\circ}\text{C}$ until incubated at 22°C for a maximum of two weeks with regular inspections, incubation temperatures chosen were $\pm 7^{\circ}\text{C}$ from maximum documented temperatures within caves to hasten growth. Plates exhibiting coverage of $>80\%$ surface area prior to two weeks were removed for refrigeration until preparation for testing.

The design preceded a methodological review. In absence of mycological expertise required for taxon identification, genetic profiling of samples was considered a prompt and accurate representation of microbial communities.

3.4. SAMPLE PREPARATION AND TESTING.

3.4.1. BONE MICROSCOPY

All bones collected from sites CR-5U56, LO-5U34 and SP-5U35 were evaluated for indications of degeneration using optical microscope NIKON SMZ25 for environmental analyses. Nine samples displaying modification were chosen for histological preparation and microscopy on the Quanta 450 scanning electron microscope (SEM). Adelaide Microscopy sectioned, carbon coated and mounted bone segments for topographical imaging with (SEM) using back scattered electrons (BSE). The diaphysis of three bones were chosen for varying superficial microbial presence, cut into thin transects and set in resin for structural.

3.4.2. CAVE ENVIRONMENT

Seven sediment samples (three each from CR-5U56 and SP-5U35; one from LO-5U35), were airdried for 68 hours at room temperature. The pH probe and meter were calibrated as per directions for Hanna HI99121 and HI1292D. Sediment was weighted to 10 g each and prepared with 25 ml of soil preparation electrolyte solution, HI7051 before measurement.

Environmental data for temperature, hydrology, humidity, and entrance structure will be assessed from previous studies at Naracoorte and based on observations made in the field around environmental parameters. other studies. Few studies have previously described these caves.

Tourist information for Blanche cave and Victoria Fossil Cave, 2019, is provided by Thomas Shortt at Naracoorte Caves National park with permission from National Parks and Wildlife Service South Australia.

3.4.3. ATMOSPHERIC GDNA PROFILING

Atmospheric- Each nutrient plate was flushed with 2 ml of reverse osmotic Milli-Q water to prevent microbial contamination. The solution was spread around the growth on the plate into a slurry and 1 ml of slurry from each plate was pipetted into a 5 ml sample tube allocated to each respective cave zone. As microbial growth is only an indicator of an ability to be cultured, flushing the plate enables inclusion of captured spores unable to grow on the selected medium.

3.4.4. SOIL, BONE AND FAECAL PELLET GDNA PROFILING

A femur and tibia from experimental sites in CR-5U56 and LO-5U34 were selected to maintain continuity with soil testing. Sediment was scraped from underneath the site of the respective bone and secured in air-tight specimen vials. Two grams of each soil sample was transferred to a 5 ml vial. A 2 mm wide transect of both bones was cut along the diaphysis, crushed and 2 grams of each was transferred into 5 ml vials. Debris from both medullary cavities was included in the samples.

For fungal profiling only - one gram of fungi was collected from the CR-5U56 scapula and secured within a 50 ml specimen jar. Faecal pellets were delivered within original collection jars.

PCR amplification of targets 16s 341F-806R and ITS (Internal Transcribed Spacer): 1F-

2R were conducted using primers specified by the AGRF, then sequenced on the Illumina MiSeq platform for bacterial and fungal identification within total 23 samples; air, bone, faeces and soil. Bioinformatics were provided by the AGRF using the basic local alignment search tool (BLAST) for identification and qualification of Operational Taxonomic Units (OTUs).

All sample preparations for molecular analysis were performed within a laminar flow cabinet with adherence to sterilisation procedures to minimize sample contamination. Specimens were delivered on ice to the Australian Genome Research Facility (AGRF) for nucleic acid extraction and gDNA diversity profiling.

4. OBSERVATIONS AND RESULTS

4.1. MICROSCOPY

LO-5U34 (Figure 3) bones were ~3 m from entrance, within twilight zone. Skeleton had been disarticulated early and dispersed by consecutive pitfall victims (Reed 2009). Experimental Tibia from LO-5U35 was imaged using the Quanta450 SEM. Distal region of tibia (Figure 7.a and 7.e) displays dark staining and corrosion from contact with acidic sediment (Fernandez-Jalvo 2016). Proximal end of tibia was subaerial with no contact to the sediment and appears less corroded. The cavity of the nutrient foramen (Figure 3.a) displays organic phototrophic (Hospitaleche et al. 2011) growth and fine cracks appear alongside organism. Magnification of region next to nutrient foramen (Figure 3.b) on exterior bone surface indicates widening of pores and increased pitting with removal of periosteal cortex. High magnification of surface pit (Figure 3.d), shows numerous vegetative bacterial cells amongst bone debris within a crack which forms in a corroded pit (Behrensmeyer 1978, Fernandez-Jalvo 2016, Golubic et al. 1975,

GómezCornelio et al. 2012). The transect (Figure 3.f) from distal shaft from shows no characteristic bioerosion. Pitting along outer edge of cortical surface and widening of internal canals indicates environmental corrosion and elemental leaching of inorganic elements, discolouration, from the bone due to wet environments and soil pH (Fernandez-Jalvo 2016). Excessive cracking of transect may be due to structural instability exacerbated by incorrect histological procedures. No bacterial MFD or Wedl tunnels are noted.

CR-5U56 (Figure 4) femur was collected ~50 m from entrance within dark, humid zone. Putrefaction occurred quickly and carcass had extensive fungal coverage (Figure 4) (Reed 2009). Bones were stained brown by decomposition fluid (Figure 4.a) (Jans 2008, Paczkowski and Schütz 2011, Behrensmeyer 1978, Fernandez-Jalvo 2016, FernándezJalvo et al. 2010). Both metaphysis and epiphysis regions appear to have lost cortical bone and reveals spongiform structure of bone. Corrosion affects the outer periosteal layer of bone around pores (Figure 4.b) due to extended contact with decomposition fluid or leaching from pores, pores are irregular in size (Fernandez-Jalvo 2016). Magnification of pores (Figure 4.c) reveals extensive corrosion, cracking and fungal protrusions through bone by bundled and branched hyphae. Degraded bone around hyphae is extensive and appears chalky (Marchiafava et al. 1974). Transect of tuberosity from mid-section of diaphysis (Figure 4.d) shows large and irregular increase in size of Haversian canals, discolouration from mineral leaching and considerable evidence of Type I Wedl tunnels extending inward from the outer margins of the bone characteristic of fungal bioerosion (Gómez-Cornelio et al. 2012, Popovic et al. 2015).

CR5-U56 (Figure 5) Scapula was collected by Reed and Bourne (2019) near entrance within twilight zone. The decomposition history is unknown. Bone was covered in sediment and thick white fungal hyphae (Figure 5.a). A sample near the spine of the scapula was selected for presence of hyphae. Conical puncture marks, scraping and tattered edges around the lateral border indicate chewing and tooth indentation from fox predation (Fernandez-Jalvo 2016). Hypha with sediments and bone debris adhering to the chitinous cell wall (Figure 5.d) and carbon beside the hypha indicate adhesive exudates from fungi and fine cracks in the bone are directed alongside the hypha, suggesting coincided damage (Ritz and Young 2004, Jiang et al. 2017, Fernandez-Jalvo 2016). Bundled hypha within a cavity sits between the periosteal layer fibrous cortex (Figure 5.c). And, is bundled hypha extend outward from a degraded cavity (Figure 5.b). The noticeable channels and pits around the hypha example difference between natural osteoclastic resorption of bone remodelling and in figure a, and sharp edge to the side of the surface tunnel of the fungi indicates fresh damage without decalcification (Miyazaki et al. 2011, Marchiafava et al. 1974).

SP-5U35 (Figure 6) Femur with unknown deposition date appears structurally stable with a polished appearance and was collected from fan of organic matter under entrance window. Mid diaphysis was sampled. Fine fissures run lengthwise along the diaphysis and bone has been stained brown from putrefaction or humic acids (Figure 6.a) (Fernandez-Jalvo 2016, Kendall et al. 2018). Surface of patina stain shows localised cracking and flaking of periosteal bone (Figure 6. c), deposition of clay-like sediment and reveals fibrous cortical bone (Brehm et al. 2005, Hospitaleche et al. 2011, Vanderwolf et al. 2013). Transection of mid-diaphysis directs arrows toward Haversian tunnel with visible branching hypha penetrating from tunnel into surrounding osteon

widening the haversian tunnel, creating distinctive bifurcating Wedl type I tunnels (Figure 6. b). Transection of outer periosteal margins illustrates extensive bacterial infiltration characteristic of non-Wedl MFD (Figure 6.d), both linear-longitudinal (LL) and budded (BD) (Hackett 1981). There appears no cuffing from hyper mineralisation around the bacterial pits (Hackett 1981). A deep gouge penetrates to cortical bone below the periosteal layer as possible anchor site of a thallus and is beginning to sever from the bone (Fernandez-Jalvo 2016, Hospitaleche et al. 2011).

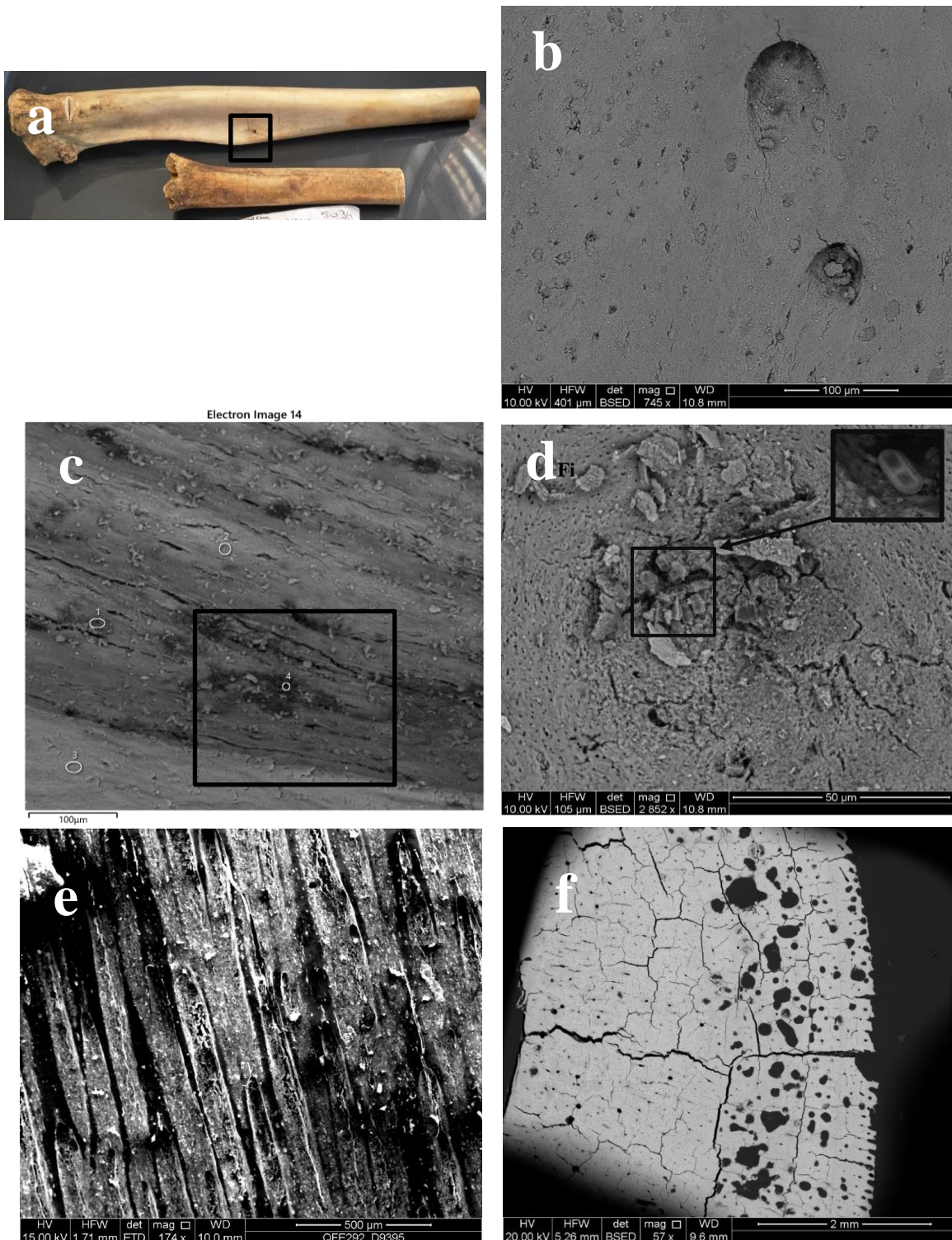


Figure 3: a) LO-5U34 Experimental tibia deposited in 1998 by Reed (2009). Black square = sample area. b) Arrows point to corroded pits on area around nutrient foramen. c) Inside entrance of nutrient foramen. Square= organic growth with fine cracking on either side of growth. d) Area on cortical surface near nutrient foramen. Arrows indicate an increase of porosity around Volkmann's canals by formation of small bacterially induced corrosive pits and fine cracks. d) Magnification of pits from from (d) contains debris and vegetative bacterial infiltration of central fissure within pit. e) Distal end of tibia displays extensive corrosion and staining in (a) from sediment contact with low pH. f) Transect of cortical bone from distal shaft from (3) shows no characteristic bioerosion. Pitting along outer edge of cortical surface and widening of internal canals indicates environmentally influenced corrosion and elemental leaching of inorganic elements from the bone due to wet environments and soil pH.

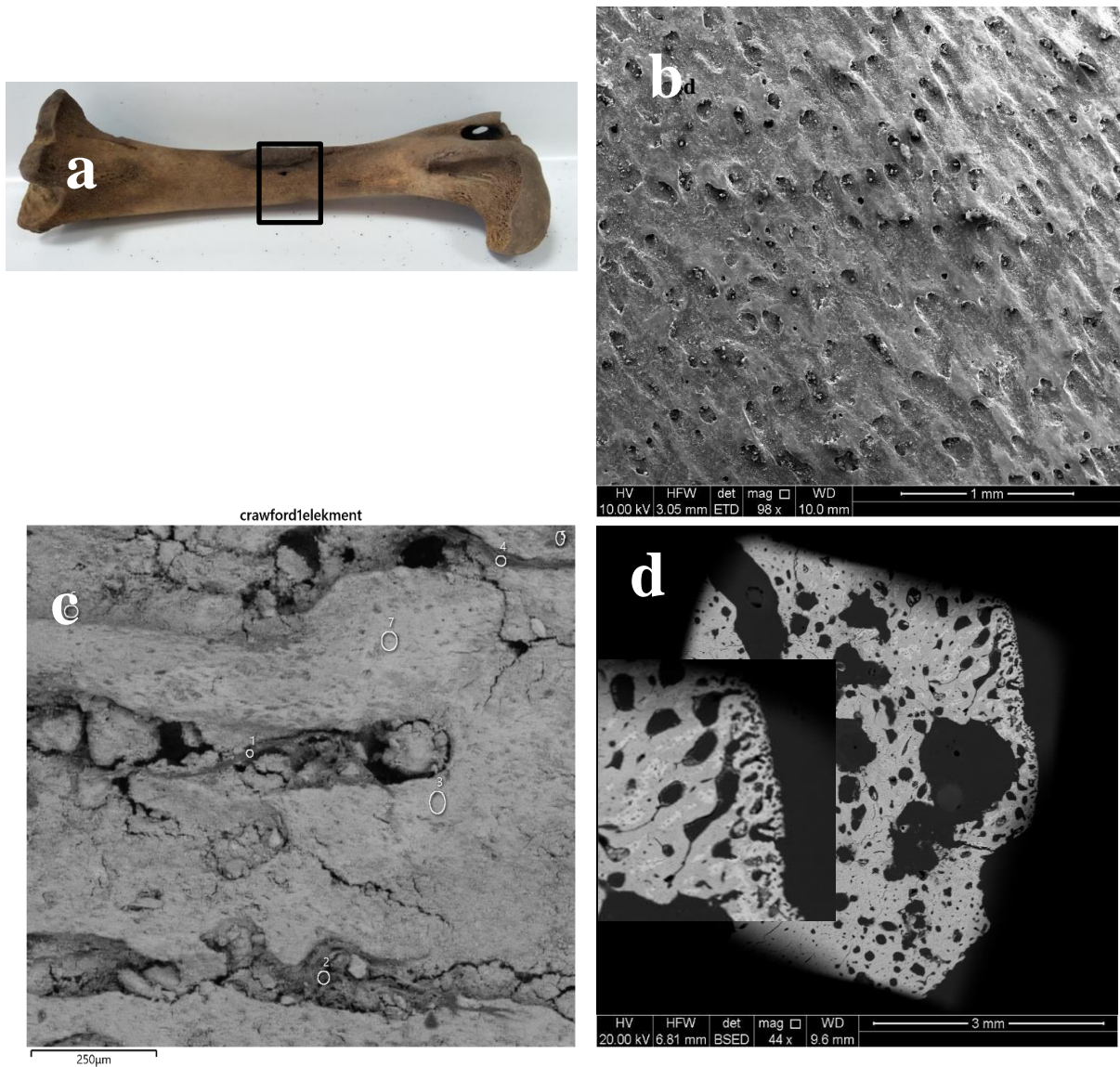


Figure 4: a) CR-5U56 Experimental femur deposited in 1998 by Reed (2009). Black square= mid diaphysis with nutrient foramen and tuberosity. Evident staining from sediment and decomposition fluid. b) Surface shows widening and sediment infilling of pores. Corrosive paths from solubilisation of surface bone surrounds pores c) Fungal hyphae with sediment attachment protrudes from punched out pores. Degradaded channels and fractures occur around hyphal extension. d) Transection of mid-diaphysis displays extensive infiltration within deltoid tuberosity. White square displays Wedl type I tunnelling from fungi, tunnels extend in ward from the cortical layer of periosteal bone Haversian tunnels are filled with fungi and debris that has been brought in from adhering to the hyphae.

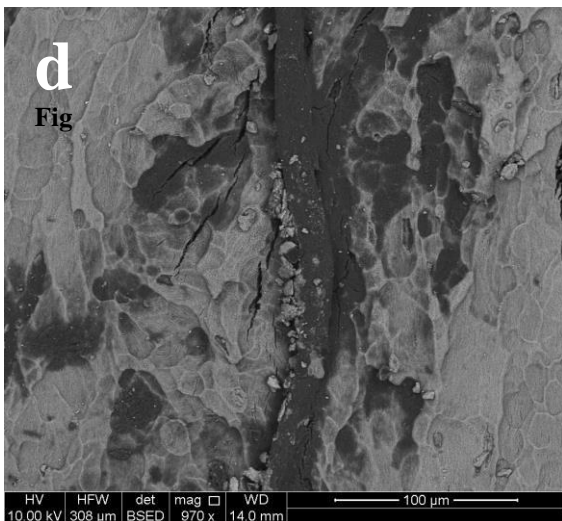
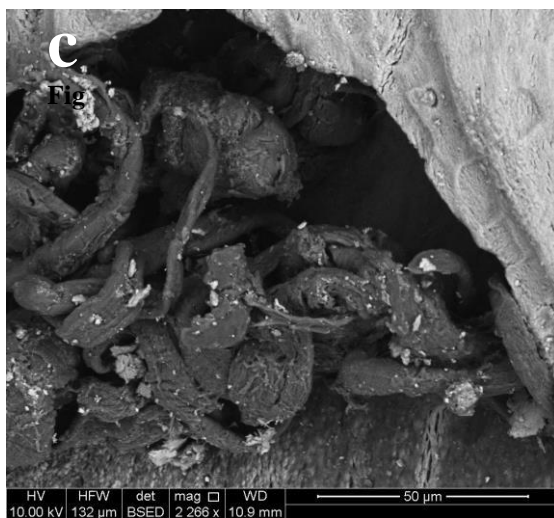
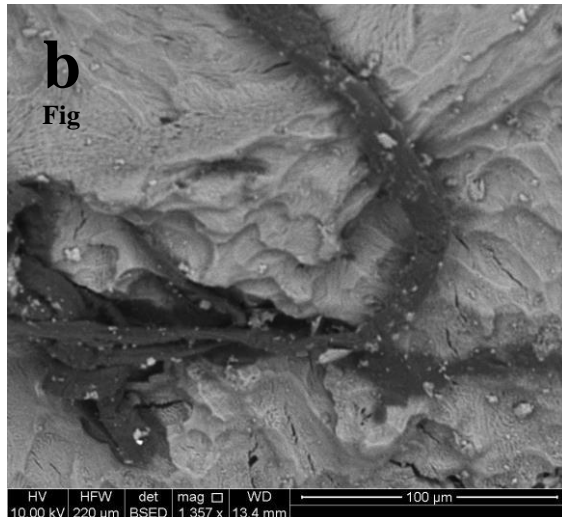


Figure 5: a) Scapula covered in fungal hypha from twilight area of CR-5U56. b) Fungal hypha protrude from cavity created within bone, c) Bundled hypha within cavity between periosteal bone and fibrous bone. d) Fungal hypha tunnel seen underneath to create sharp tunnel edges, suggesting new damage. Resorption pitting from osteoclast bone remodelling is around hypha. Debris adheres to hypha chitin layer suggesting sticky exudates.



Figure 6: a) SP-5U35 Humerus with unknown deposition date collected from area around organic sediment cone. Slightly polished exterior. Sample square = mid-diaphysis with patina. b) Transection of mid-diaphysis directs arrows toward Haversian tunnel with visible branching hypha penetrating into surrounding osteon in Wedl II tunnels. c) Magnification of staining reveals site as potential phototropic attachment with fractures, porous bone exposed and clay-like deposits. d) Transection of same sample in (b) illustrates extensive bacterial infiltration characteristic of nonWedl MFD, both linear-longitudinal (LL) and budded (BD). No hypermineralisation is seen. The surface of the perosteal cortical layer of bone is beginning to sever from the bone from severe degradation.

4.2. GDNA PROFILING AND MICROBIAL DIVERSITY

ITS markers produced six fungal phyla represented by 232 species (Figure 7)

(Appendix A). Ascomycota represents the largest diversity of OTUs (71 %),

Basidiomycota (22.94 %) and Glomeromycota, Mortierellomycota, Mucormycota, Rozellomycota and unidentified OTUs contribute a combined total of 6.07 % (Figure 9).

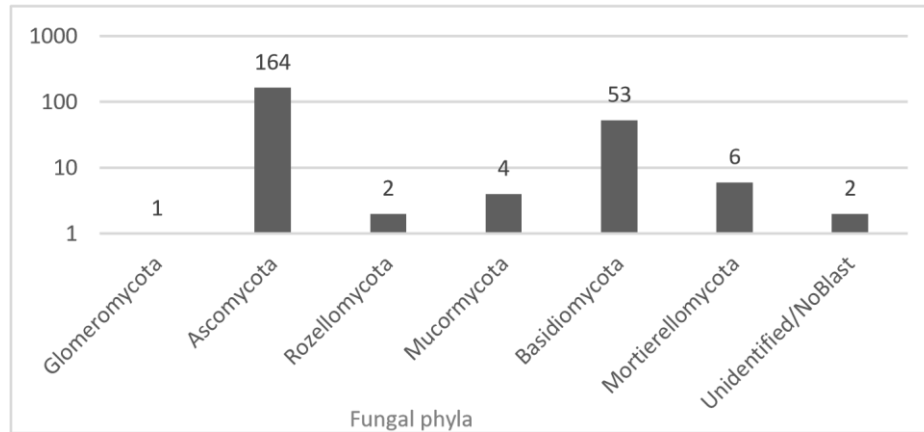


Figure 7: Logarithmic scale of Fungal diversity from gDNA profiling of phyla at Naracoorte Caves. Samples collected from VF-5U1, CR-5U56, BL-5U4,5,6, LO5U34.

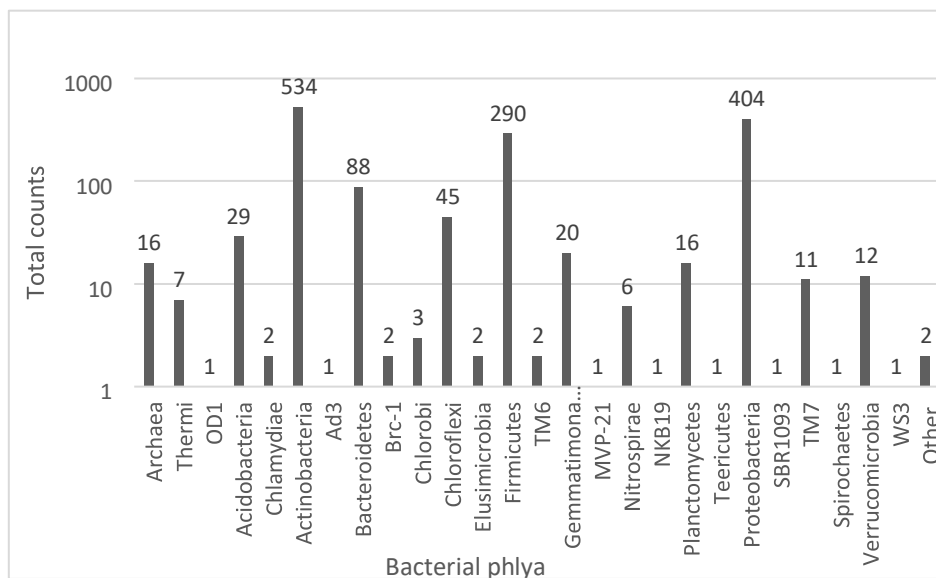




Figure 8: Logarithmic scale of Bacterial diversity from gDNA profiling of phyla at Naracoorte Caves. Samples collected from VF-5U1, CR-5U56, BL-5U4,5,6, LO5U34

Table 1: Species list for gDNA profiling of fungi and bone and faeces samples from CR-5U56 and SP-5U35.

Cave	5U35 Specimen			5U56 Crawford's dead sheep		
	~1m diameter solution pipe, ~2m deep. Grate over entrance. Sediment cone with abundance organic detritus. Humid, low temperature.			Open, horizontal window ~4m width, ~1m high. Walk-in. Vvinyard on private property. >90% humidity in rear chamber, 1416°C		
Entrance type						
Humidity & temperature						
Light	Light	Twilight	Dark	Dark	Dark	Twilight
Soil location	Adjacent entrance ladder	10m from ladder	Near excavation pit ~30m from ladder	Under exp. Skeleton(2009), rear chamber	Under Echidna skeleton, rear chamber	Under bones, midchamber decoration
Soil site	SP1	SP2	SP3	chamber CDS1	CDS2	n CDS3
Soil pH	7.34	8.24	8.85	7.88	7.57	8.79
Sample						
Taxon	a) Faeces covered in hyphae			b) Hyphae in faeces	c) Scapula with fungal hyphae	
Penicillium_atramentosum		0.30%		18.60%		0.00%
Penicillium_expansum		41.10%		0.00%		0.00%
Gymnoascus_reessii		0.00%		0.10%		12.50%
Onygenales;s_unidentified		0.00%		2.40%		7.70%
Beauveria_felina		0.00%		72.00%		58.60%
Monocillium_tenuis		1.30%		0.00%		0.00%
Dactylonectria_estremocensis		3.00%		0.00%		0.00%
Nectriaceae;s_unidentified		4.00%		0.00%		0.20%
Gamsia_simplex		0.00%		2.20%		10.70%
Candida_railenensis		1.40%		0.00%		0.00%
Tausonia_pullulans		4.40%		0.00%		0.00%
Solicoccozyma_aeria		14.90%		0.00%		0.00%
Solicoccozyma_phenolica		12.50%		0.00%		0.00%
Saitozyma_podzolica		2.10%		0.00%		0.00%
Cutaneotrichosporon_guehoae		5.80%		0.00%		0.00%
Cutaneotrichosporon_smithiae		0.00%		2.90%		0.20%
Mortierella_polygonia		0.00%		0.90%		4.50%
Other/Unidentified/No blast		9.00%		0.80%		5.10%

ITS results from the scapula and faeces produced 138 fungal OTUs with 85 from CR5U56 the scapula, 41 from CR-5U56 faecal sample and 56 from SP-5U35 faecal sample (Appendix A). Species recovered were comprised of Ascomycota (82.5 %), Basidiomycota (15.1 %) and Mortierellomycota (1.8 %).

16srRNA markers generated 475 bacterial OTUs across 30 phyla (Figure 8). The dominant phyla were Proteobacteria (29.3 %), Actinobacteria (21.5 %) Firmicutes (17.3%) and Bacteroidetes (7.4 %) Chloroflexi (5.7 %). The remaining 23 phyla contribute 18.8%.

Distribution of diversity throughout VF-5U1 indicates Area 10 had the highest diversity of taxa across all air samples (Table 2) within both caves, for fungi (53) and bacteria (124).

Total microbial diversity in BL5U4,5,6 was highest in Area 1 for bacteria (70 species), while the highest fungal diversity was in Area 3 (45 species). A steady linear decrease in bacterial richness is seen from the main entrance of BL-5U4,5,6 to the rear chamber. Fungi follow this trend but increase slightly in Area3 (Table 2)

Calculating mean average was to compensate for unequal sampling between caves, indicate BL-5U4,5,6 has a larger diversity of microbes than VF-5U1; bacteria (\bar{x} 53.5 > 50.3) and fungi (\bar{x} 32 > 14.6).

Table 2: Species diversity abundance for bacteria and fungi in gDNA samples from atmospheric samples in VF-5U1, BL-5U4,5,6; and soil and bone samples from LO-5U34 and CR-5U56.

Victoria fossil VF-5U1 Atmosphere				
		Species count		
Sample no.	from entrance	Fungi	Bacteria	Total
VI-5	Area 1 HD	28	63	91
VI-1	Area 2 HD	7	49	56
VI-10	Area 3 LD	7	41	48
VI-4	Area 4 HD	6	62	68
VI-3	Area 5 LD	12	42	54
VI-8	Area 6 HD	5	45	50
VI-7	Area 7 LD	8	39	47
VI-2	Area 8 LD	8	31	39
VI-9	Area 9 LD	12	60	72
VI-6	Area 10 HD	53	71	124
TOTAL:		146	503	649
Mean average:		14.6	50.3	64.9
Blanche BL-5U4, 5, 6 Atmosphere				
		Species count		
Sample no.	from entrance	Fungi	Bacteria	Total
BL-2	Area 1 HD	43	70	113
BL-5	Area 2 HD	28	65	93
BL-6	Area 3 LD	45	63	108
BL-3	Area 4 HD	36	54	90
BL-1	Area 5 LD	22	44	66
BL-4	Area 6 LD	18	25	43
TOTAL:		192	321	513
LO-5U35 (entrance) and CR-5U56 (rear) Soil & Bone				
Location	Sample	Fungi	Bacteria	Total
LO-5U34	Soil	146	342	488
LO-5U34	Bone	5	34	39
CR-5U56	Soil	60	279	339
CR-5U56	Bone	5	21	26
Total:		216	676	892

One way analysis of variance (ANOVA) tested significance between high disturbance (HD) and low disturbance (LD) sites in VF-5U1 and BL-5U4,5,6, concluding no significance in the abundance of atmospheric bacteria and fungi within HD and LD areas within caves. Bacterial abundance between VF-5U1 and BL-5U4,5,6 was also not

mathematically significant. However, differences in fungal abundance was significant between VF-5U1 and BL-5U4,5,6, (F-statistic value = 5.988, $p = 0.0282 < 0.05$).

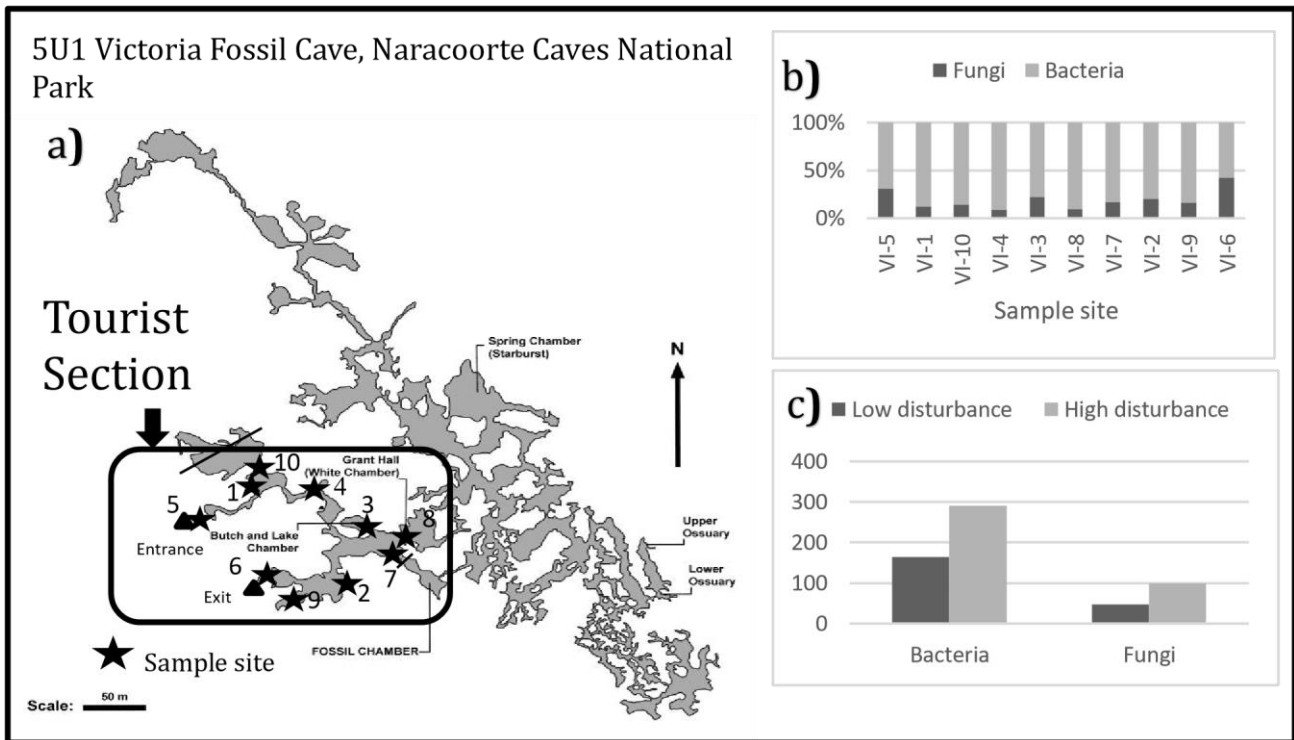


Figure 9: VF-5U1 sample site map a) Atmospheric microbial settle plate sampling sites depicted on tourist map of Victoria Fossil Cave for bacteria and fungi in high disturbance (HD) and low disturbance (LD) areas. b) Site comparison for bacteria and fungi diversity c) Diversity comparisons between high disturbance and low disturbance zones.

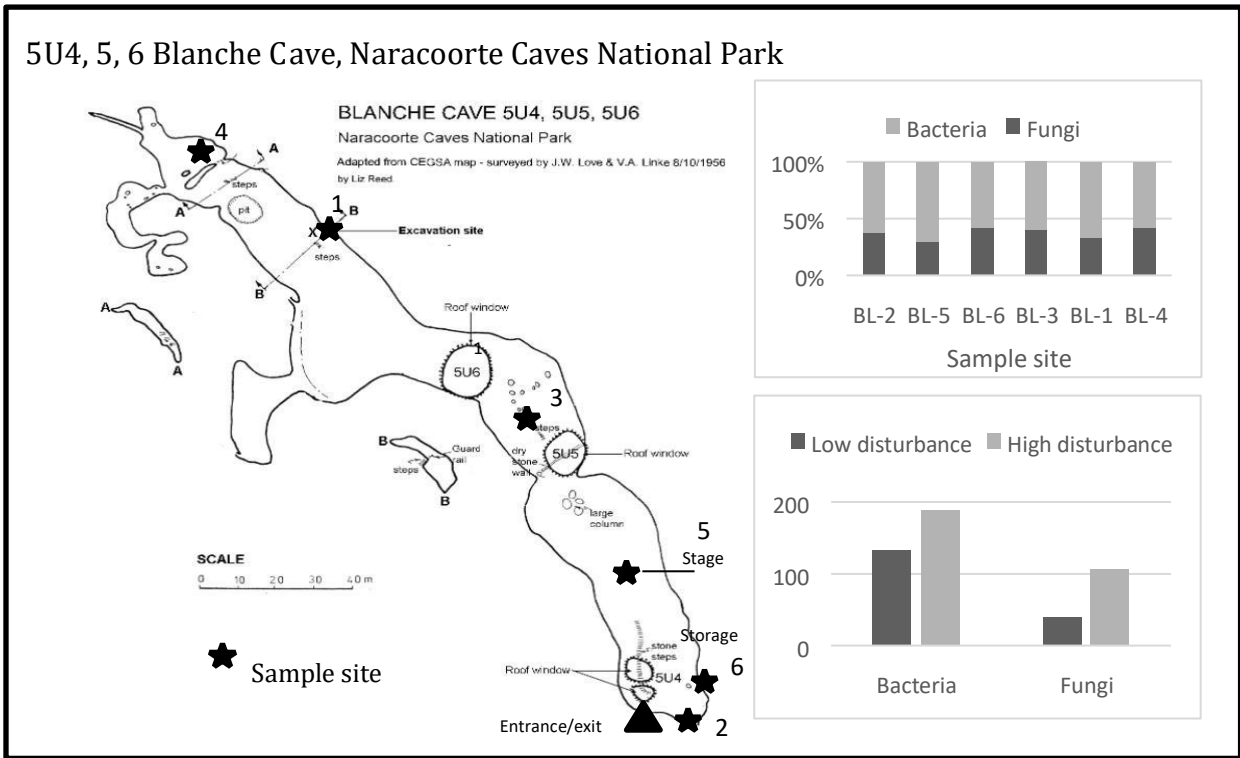


Figure 10: a) Atmospheric microbial settle plate sampling sites depicted on tourist map of Blanche Cave for bacteria and fungi in high disturbance (HD) and low disturbance (LD) areas. b) Site comparison for bacteria and fungi diversity c) Diversity comparisons between high disturbance and low disturbance

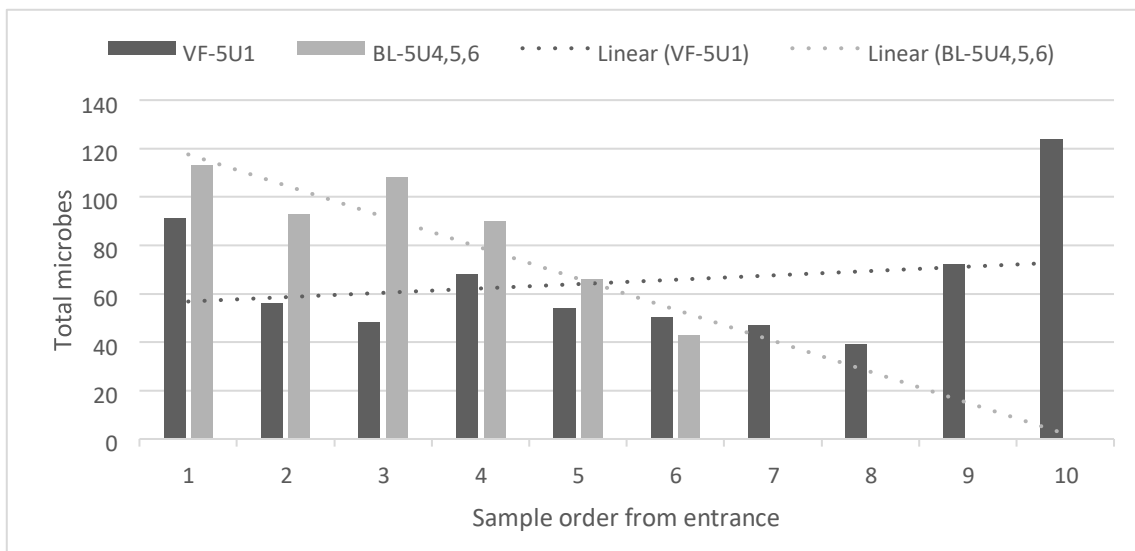


Figure 11: Linear regression analysis of total atmospheric microbes in VF-5U1 and BL-5U4,5,6 in sample order as distance from entrance. VF-5U1(R=0.04) and BL-5U4,5,6 (R=0.816909).

Experimental soil samples taken underneath decay sites from CR-5U56 and LO-5U34 produced highest diversities of fungi with single samples. LO-5U34 had 81 exclusive fungi from Ascomycota, Basidiomycota, Mortierellomycota and Rozellomycota. And, 92 unique bacteria within a total of 342 across 17 phyla. Most bacteria are Proteobacteria, Firmicutes, Actinobacteria, Chloroflexi, Verrucomicrobia and Bacteroidetes. The overall total fungal diversity was 146 species.

CR-5U56 has a total of 60 fungal OTUs, contributing 12 unique species in Ascomycota and Basidiomycota. And, 31 unique bacterial species are across 10 phyla, including: Actinobacteria, Proteobacteria and Bacteroidetes.

Modern bones collected from the soil samples returned the least OTUs, with 5 fungal in both the tibia and the femur. All 5 fungi in the tibia are from Ascomycota. The femur from CR5U56 were from Ascomycota and Basidiomycota. Bacteria diversity from the bones was higher in the LO-5U34 tibia, 34, and CR-5U56, 21, within; Actinobacteria, Firmicutes, Proteobacteria, Bacteroidetes, Firmicutes, Tm7 and Cyanobacteria.

Cluster analysis with Non-metric Multi-dimensional scaling (MDS) and Kulczynski group averages of all microbial samples (Figure 12) determined high dissimilarity between species within individual cave sites and between caves, <45% overall similarity between caves. BL-5U4,5,6 had the highest similarity between sample sites (<80%). Microbial phyla, primarily Firmicutes (Bacillales), Actinobacteria, Bacteroidetes and Cyanobacteria, and fungi, Ascomycota, showed the highest similarities (appendix). While VF-5U1 sites shows similarity in sample no. VI-3, VI-8, VI-2 and VI-7, this occurred within the main fossil chamber. And, VI-1 and VI-4 are popular areas to stop along the tourist path. VI-5 was a control from outside of VF-5U1

and displays the most similarity (~40%) with BL-5U4,5,6. Meanwhile, BL-5U4,5,6 showed a clear division in similarity between three samples closest to the main chamber entrance and the farthest.

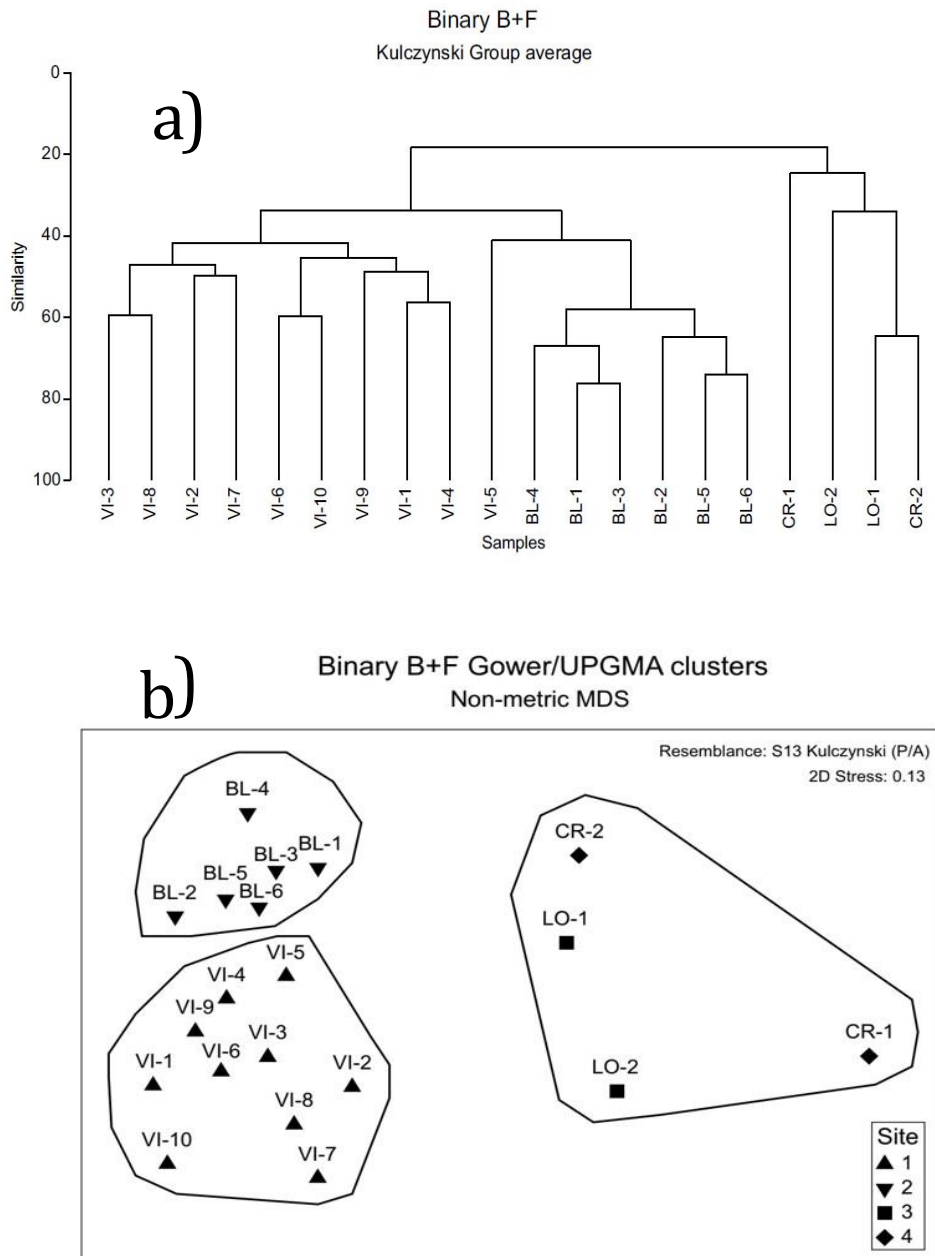


Figure 12: Cluster analysis with Non-metric Multi-dimensional scaling (MDS) and Kulczynski group averages for dissimilarity testing. gDNA samples were given sample names by AGRF, they do not represent order from entrance, but represent each zone for VF-5U1 (Figure 9) and BL-5U4,5,6 (Figure 10). Caves show distinct communities of microbes. a) Distance representation for % of similarity between sites. b) Cluster analysis.

4.3. CAVE ENVIRONMENT ASSESSMENT

4.3.1. BLANCHE CAVE (BL-5U4,5,6)

Site BL-5U4,5,6 (Figure 13) has three roof collapse windows (Figure 13 a.b.c.), with extensive light zones, dynamic air flow and a relatively dry environment. Hydrological input to sediment cones during wet seasons enables vegetation (Figure 13.c) and phototrophic microbial growth (Figure 13. a). Temperatures fluctuate with seasonal variation from 8-15° C and relative humidity ~50-75% (Sanderson and Bourne 2002). The dry conditions have caused desiccation of deceased animals and organic matter (Figure 13. d). Nutrients are imported by passive air flow, water and by animals that use the cave to scavenge or for shelter (e.g. possums, rodents). Pleistocene fossil deposits within the cave largely accumulated via owl pellet deposition from roosting Masked and Barn Owls (Macken and Reed 2013). Blanche cave has been used for entertainment and tourism since 1845, with 2019 documenting ~6400 visitors (Thomas Shortt pers. comm. 2020).

4.3.2. VICTORIA FOSSIL CAVE (VF-5U1)

Site VF-5U1 (Figure 14) has two closed artificial entrances (Figure 14.d) that lead to excavated and natural passages (Figure 14.d) with low chambers decorated with speleothems and the main fossil chamber, with a ceiling <4m high (Figure 14.c). Temperatures are stable at 16-19° C (Sanderson and Bourne 2002) and closed entrances prevent natural light and evaporation of moisture; therefore, the cave is completely dark apart from artificial lights. Relative humidity remains above 90% with moderately static atmosphere and hydrological input restricted to vadose flow (Sanderson and Bourne

2002). Disturbance to airflow is only created through the doors and by movement of people through the cave. The fossil bed is on a low floor separated from the general viewing area and only accessible to researchers and cave management (Figure 14.a). Human visitation is the main source of allochthonous input with 18,861 documented tourists in 2019 (Thomas Shortt pers. comm. 2020). Since the natural pitfall entrances for the fossil deposit closed approximately 213 Kya (Liz Reed pers. Comm. 2020), only invertebrates and small vertebrates (e.g. rodents and reptiles) can access the cave for shelter, with cave crickets (*Novotettix naracoortensis*) congregating by the rear passage, making VF-5U1 extremely oligotrophic.

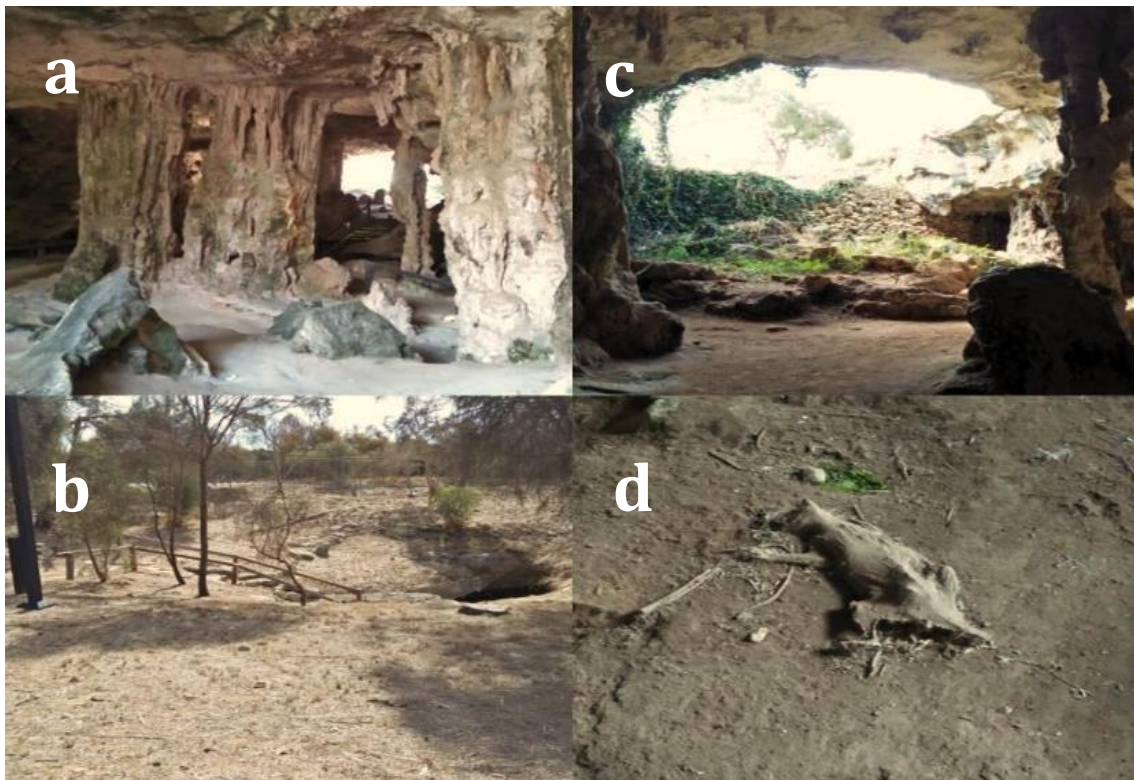


Figure 13: BL-5U4,5,6 a) Phototrophic microorganisms near light zone of entrance 5U4 create green film within porous limestone of cave structures. b) Slump of roof collapse funnels organic matter, water and directs airflow into main entrance chamber from entrance 5U4. c) Window 5U5, sediment cone displays nutrient and hydrological input sufficient to support plant growth within photic zone. d) Desiccated possum near entrance 5U4 caused by reduced microbial decomposition within an arid environment inducing mummification of soft tissue. Green phototrophic organisms grow around moisture of speleogenic drip in light zone.

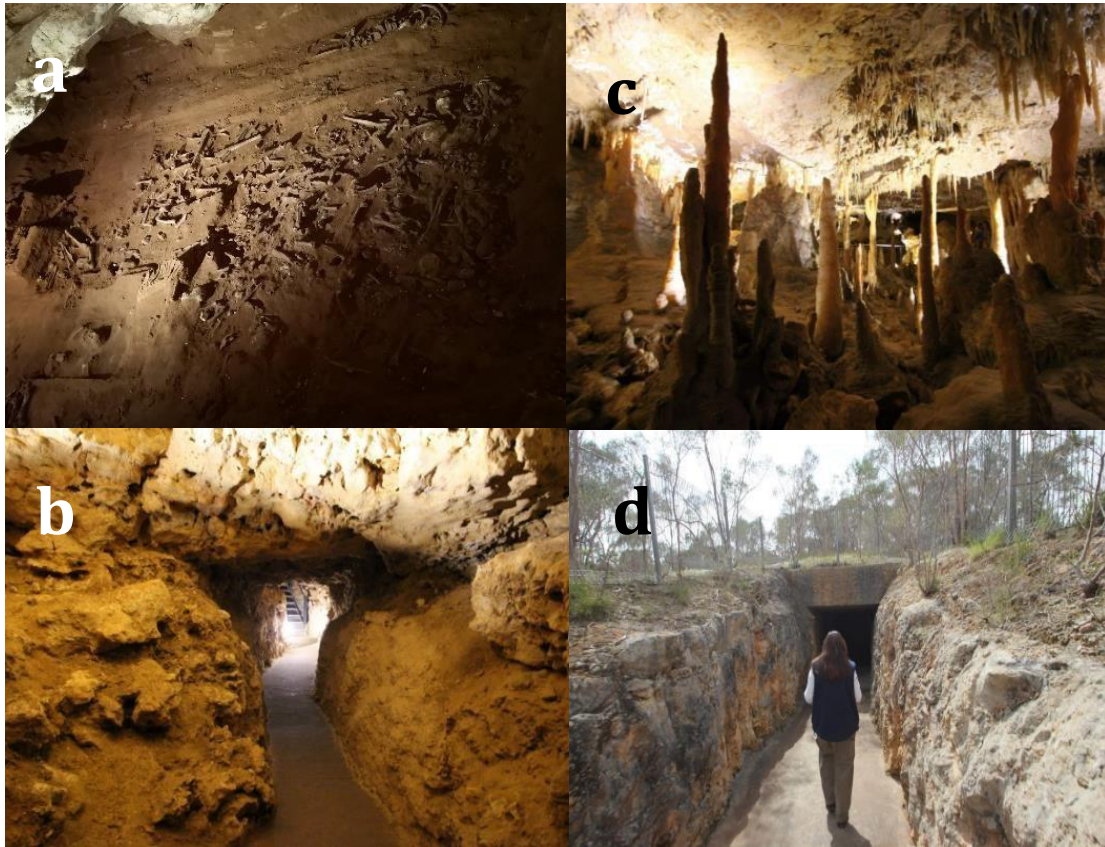


Figure 14: VF-5U1 a) Exposed fossil bed below viewing platform in main tourist chamber. The fossil bed displays numerous bones from the middle Pleistocene. b) Narrow renovated tourist path through limestone minimises air flow from connected chambers. Air flow is directed by visitor disturbance. c) Albert Edward grotto. Calcareous speleothems form by hydrological input from rainwater in soil. d) Surrounded by native landscape, a constructed entry point is sealed by a door to maintain security and within-cave environments. Cave is only illuminated by artificial lighting. [Victoria Fossil Cave. (2020). Images retrieved from <https://www.mountgambierpoint.com.au/attractions/victoria-fossil-cave/>].

4.3.3. CRAWFORD'S DEAD SHEEP CAVE (CR-5U56)

Site CR-5U56 (Figure 15) is adjacent to NCNP on private viticultural land, the horizontal entry is ~4 m in width and 1 m in depth (Reed 2009). Low ceilings and narrow crawl spaces are decorated with speleothems and proceeds ~40 m to a rear chamber, the cave being ~60 m in length (Figure 15.c) (Reed 2009). The nature of the entrances obstructs airflow, hydrological input and light from the entrance, so the atmosphere in the inner chamber is static and humid at >90%, with temperatures of

1416° C (Reed 2009). Relatively undisturbed, the entrance area has been visited by foxes and scavengers, evident by fresh bones of smaller mammals and sheep with puncture marks and gnawing. The rear chamber remains undisturbed apart from insects, reptiles, and possible rodents. The rear chamber of CR-5U56 was used for decomposition studies by Reed (2009) in 1998-2001 (Figure 15.a and 15. b) and the kangaroo skeleton placed during that study remained undisturbed within the original site of deposition (Figure 15.c) . pH from sediment samples are: CDS1, underneath kangaroo experiment 7.88, CDS2 7.57 and CDS3 8.79.

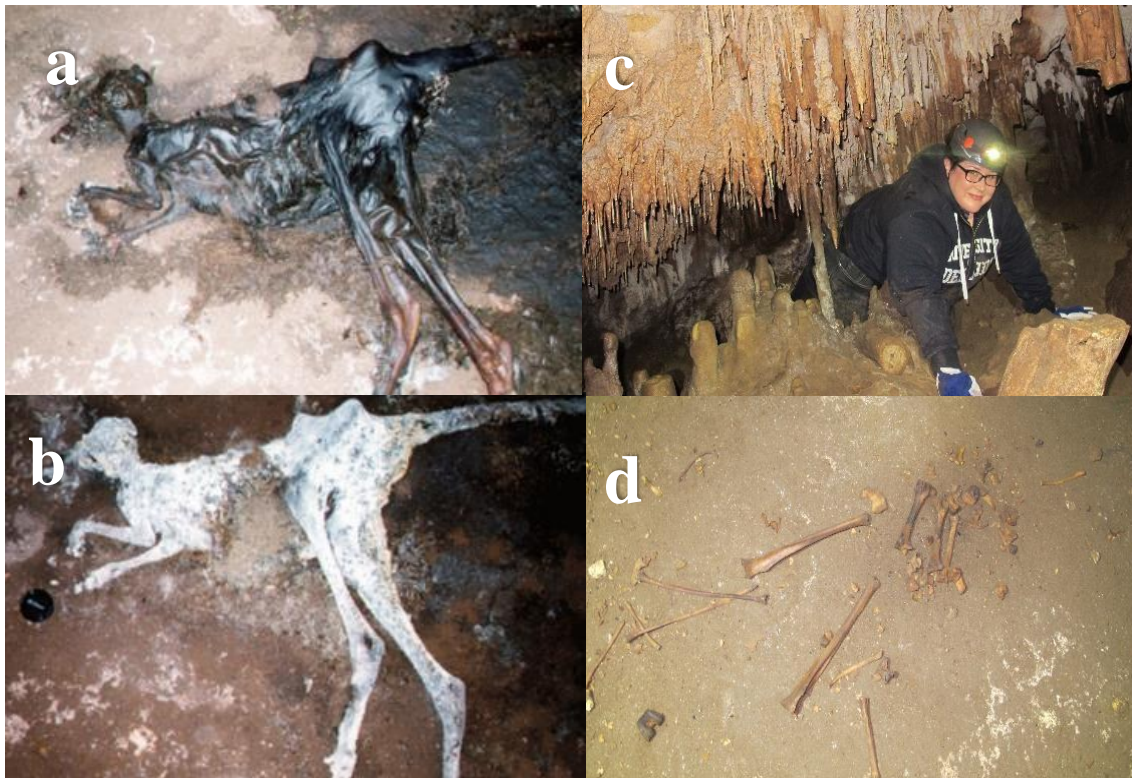


Figure 15: CR-5U56 a) Day 14 decomposition of Western grey kangaroo in humid rear chamber, experiment by Reed (2009) shows quick putrefaction b) Day 194 of decomposition skeleton and leaching of decomposition acids into soil (Reed 2009). c) Speleothems decorate the mid-section of the cave between the entrance and the rear chamber (Bourne 2020). d) Skeletal remnants of the Western grey kangaroo (Reed 2001) appear blackened from fluid staining (Bourne 2020)

4.3.4. LOST CAVE (LO-5U34)

Site LO-5U34 (Figure 16) is located within native scrubland adjacent to NCNP and has little visitation from humans. It has a roof collapse window entrance, with a steep floor descending 4 m from the window and extending into 40 metres of chambers and passages (Reed 2009). Temperatures and humidity have been comparatively described by Reed (2009) as analogous to Robertson Cave as 8-15°C with a mean of 11.94 °C and 80-110% humidity with seasonal variability (Sanderson and Bourne 2002). Due to the proximity of scrub and slumping from the entrance, the allocthonous input is extensive within the light and twilight zone, with evidence of moss, algae, and ferns. Lost cave is an effective pitfall trap with evidence of multiple wallabies, indicating a high degree of decomposition and nutritional input. Lost cave was a comparative location for Reed's 2009 study, albeit trampling from consecutive pitfall victims has disarticulated and dispersed the original experimental bones over the last 22 years (2009). pH from underneath kangaroo experiment was 6.71.



Figure 16: LO-5U34 a) Day 14 decomposition of Western grey kangaroo in entrance chamber within twilight zone, experiment by Reed (2009). Bloat stage of decomposition and white hyphae of fungi is growing on legs. Sediment floor displays organic debris underneath kangaroo. b) Day 192 of decomposition skeleton. Skeleton has been disarticulated by consecutive pitfall victims trampling the kangaroo. Bone is covered in fungi (Reed 2009). c) The remaining bones have been scattered within the chamber, the tibia was collected for taphonomic identification. On distal end of tibia touching the sediment floor, algae are notable. d) Pelvic girdle of Western grey kangaroo and associated rocks are covered in green algae.

4.3.5 SPECIMEN CAVE (SP-5U35)

Site SP-5U35 is located on private property adjacent to NCNP. It has a 2 m deep solution pipe entrance ~1m in diameter (Liz Reed pers. Comm. 2020). Underneath the solution pipe, is a sediment cone with abundant decaying organic detritus creating by slumping at the entrance. The ceiling is ~ 5m at the highest point and the cave is approximately 50 m in length prior to a possible sediment cone that infilled a previous pitfall entrance. Pleistocene fauna was discovered within the cave in 1908 (Reed 2012)

and now the cave now has a locked hatch over the entrance to prevent visitation.

Medium sized animals such as possums are still able to access the cave between the bars, modern bones, and animal scats on the sediment floor and within the organic debris of the sediment cone indicate ongoing visitation and/or pitfall entrapment. There are minor convection currents within the cave from airflow into the caves and the cave is described as humid with low temperatures; however, there is no formal data. pH from sediment samples are: SP1 7.34, SP2 8.24 and SP3 8.85.

5. DISCUSSION

5.1. BONE TAPHONOMY AND MICROBES

Bioerosion from phototrophic microbes, fungi, and bacteria, were all represented within the bones regarded in this study: pitting and tunnelling of cortical bone and periosteal surfaces were consistent with Wedl's (1864), Hackett's (1981) and Machiafava's (1974) observations.

Fungi was the typical form of bone bioerosion which is displayed on all presented bones from CR-5U56 and SP-5U35, corresponding with Jans *et al.* observations (2004).

Regardless of similar fungal coverage observed on the kangaroos by Reed (2009) in both LO-5U34 and CR-5U56, the tibia had no evidence of fungal hypha or bacterial MFD.

Although, a phototrophic organism, potentially cyanobacteria, is seen on LO-5U34 and characteristic markings on SP-5U35 both occurring on bones from within the low photic zone. Cyanobacteria was detected on CR-5U56, although not expressed.

Both kangaroos remained intact during early decomposition but did not display characteristic MFD, contrary to Jan's (2004) correlation between dismemberment or scavenging and lack of bacterial MFD. Therefore, it is possible that bacterial MFD may be delayed through environmental factors, such as desiccation within dry soils and dynamic airflow of the open cave LO-5U34. Or, by limiting factors that affect bacterial growth during putrefaction, seen in CR-5U56 (Janaway et al 2009, Marquez-Grant et al. 2017, Paczkowski et al. 2011).

Corrosion of the distal end of the tibia is suggestive of the acidic pH of the soil; however, soil corrosion can be mistaken for bacterial erosion (Turner-Walker 2019). Regardless of the lack of MFD within the tibia, there was a high diversity of bacteria of which are still associated with early putrefaction, most notably *Clostridium*, *Lactobacillus* and *Bacteroides* (Appendix A)(Marquez-Grant et al. 2017). However, the bacteria within CR-5U56 femur coincided with bacteria associated with ~4 years post decomposition of the skeletal stage: Firmicutes, Actinobacteria, Alpha and Gamma proteobacteria (Appendix A) (Marquez-Grant et al. 2017). This may reflect the diversity of bacteria within the LO-5U34 soils. However, if growth limiting factors have delayed earlier stages of microbial decomposition, or are dormant, this may contribute to the low amount of bioerosion from fungi and bacteria, and enabling the onset of the better-adapted phototrophic organisms within environmental extremes of LO-5U56 (Wisshak 2012). Moreover, if bacteria are dormant and can be provoked by favourable conditions seen in the temperature increases that inspired fungal activity within SP-5U35 and CR-5U56 within photic zones, this may provide another theory for delayed bacterial MFD (Stuart and Jay 2010), separate to post-burial soil microbes.

SP-5U35 is an interesting contradiction between macroscopic preservation and microscopic bioerosion. The rare combination of fungal and bacterial bioerosion (Jans et al. 2004) in the femur may indicate a previous lichen-like symbioses; however, no previous research has provided descriptions of MFD with Wedl tunnels as a singular symbiotic event. Although this rarity warrants further investigation, the dual microbial presence and the phototrophic degradation on the surface were considered as a separate occurrence for this study. The differences in fungal diversity and tunnelling between SP-5U35 femur and CR-5U56 femur indicate that size and type of tunnel is feasibly species-related. This is supported by vast differences of species within the SP-5U35 faeces opposed to the CR-5U56 faecal/scapula and is a potential indication of the unique community found in SP-5U35 (untested). The dissimilarity test of each cave and each community within the cave zones are unique in composition.

The polished look of the periosteal layer of SP-5U35, also seen in another sample (Appendix B), may indicate early permineralisation from bacterially mediated precipitation, via increased directional hydrology and presence of anaerobic bacteria within the moist organic deposits under the solution pipe (Daniel and Chin 2010, Maurer et al. 2014). This may explain the overall preservation and structural integrity of bone structure regardless of bioerosion, through reinforcement and protection.

CR-5U56 soil indicated close contact with potentially degenerative bacteria, many of which appear to be gut-related, fungi dominated samples from CR-5U56 and was seen in the tibia (Appendix B), the scapula, soil and faeces. All matched the presence of keratinophilic and chitinophagus fungi.

Although DNA presence of any microbe is not conducive to activity, as cool alkaline soils may extend DNA preservation of previous microbes (Janaway 2009), microscopy of fungal hyphae confirmed definitive presence. Fungal damage of CR-5U56 femur was not isolated, occurring in most regions micro graphed on the femoral sample and tibia (Appendix B), this indicates a wide coverage, substantiating Reed's observations (2009). The femur displayed Wedl type I fungal modifications seen in the transect and surfaces depict Marchiafava's 'punched out' holes (1975). The damage appears to corroborate Marchiafava's (1974) description of an aged infiltration, as jagged edges and extensive damage around hypha demonstrate decalcification, unlike the sharp edges around hyphal tunnelling associated with calcified bone of recent coverage, seen on the scapula. Although, the hyphae displayed on the bone and the hyphae on the faeces and dung are morphologically disparate in hyphal width. The finer hyphae imaged on the femur may be the keratinophilic Onygenales, *Gymnoascus reessii*, and consistent with Reed's documentation of fur coverage and decomposition. The femur, scapula, fungi, and soil in CR-5U56 represented *Gymnoascus reessii* (Onygenales); although this species was present in soil samples from LO-5U34 it did not appear in the bone, although may suggest that keratinophilic species may be part of an animals external biome and only become saprophytic after death.

Fungi, *Beauveria felina*, was of interest within the CR-5U56 microbial profile.

Beauveria felina is a marine derived chitinophagus insecticide and has been previously described from medical studies pertaining to bone resorption and therefore unsurprising that it dominated the scapula and faeces (Langenfeld et al. 2011, Miyazaki et al. 2011). As described on the scapula, the surface tunnels of *B. felina* are comparable to natural osteoclastic bone resorption seen around the fungi and thus could indicate a threat to

exposed vertebrate fossils. However, many fungi are able to morphologically adapt in response to environmental stress, and whilst *B. felina* may appear with robust hypha on the scapula and faeces, it is also possible that this is a response to high nutritional sources and temperature increases within the twilight zone. *Beauveria felina* is unique to CR-5U56 and, as an insecticide, is indicative of the regions anthropogenic influence from viticulture and the possible future implications on fossil preservation should infected insects migrate into other oligotrophic caves, such as VF-5U1. This also emphasizes that insects and animals (foxes etc) are contributors to the microbiota within caves.

5.2 ENVIRONMENT AND MICROBES.

Heterogeneity of species between caves and within-cave zones was significant, conveyed by the multiple testing methods. This heterogeneity may reflect disparate sampling methods; however, dissimilarity between cave sites of equal testing methods confirms unique results between caves.

In high disturbance zones of the tourist caves BL5U4,5,6 and VF5U1 human presence is reflected (Streptomyces, Corynebacterium Lactobacilli, Enterobacteria and Micrococcus), with high Bacilli in BL-5U4,5,6 and higher Enterobacteria and Pseudomonades in VF-5U1, consistent with Adetutu's (2012) data. There appeared to be an inverse relationship between the atmospheric bacterial species within VF-5U1 and the private caves (Appendix A), indicating that the diversity of VF-5U1 is closely associated with atmospheric dispersal from human disturbance.

The high diversity of fungi around the exit of VF-5U1, possibly reflecting atmospheric-driven, and human driven convection currents dragging species outward, may also be

from insect activity. It must be noted that the cave crickets congregating around the exit had partially eaten the Malt, Brain-heart and Potato dextrose agar, but not the Czapek dox, as all samples were pooled I am unable to genetically determine the difference in species occurring within each plate as a result. This is likewise within BL-5U4,5,6 within the storage area where winged insects were active, the sample also the highest fungi result in BL-5U4,5,6, but not bacteria. Therefore, it is plausible that insects encourage high dispersal of fungi within the environment, but not bacteria. The persistence of animal pathogens and heterotrophs within an oligotrophic environment reveals potentially sustained metabolic behaviours through the constant nutrient input from visitors and tourists (hair, skin, clothing lint, dung) and fungi are influenced by insects (Adetutu et al. 2011, Adetutu et al 2012).

Patterns in diversity see a decrease proximal to the entrance (in BL-5U4,5,6) and niche differences between the dominant phototrophs (Chloroflexi, Chlorobi, Cyanobacteria etc) and acidophiles in LO-5U34 and extremophiles of a static atmosphere with low airflow (Archaea, alkaliphiles, methanogens) in CR-5U56.

Adetutu (2011) and Vanderwolf (2013) associate low fungal numbers with increased tourism, though the obvious dispersal between the two private caves is a result of airflow, insect and animal activity. This is supported by differences seen between atmospheric samples in the open BL-5U4,5,6 as it decreases into the rear chamber, high diversity around HD entrances of VF-5U1 and within LO-5U56. Due to restrictions within access to caves and the timescale of this study I was unable to conclude if these atmospheric and soil diversities change during seasonal fluctuations.

Desiccative environments of LO-5U34 prevent microbial activity within soils and prevent the breakdown of lignified and cellulose allochthonous material, with increased hydrology it is possible leaching of nutrients has decreased soil pH, corroding the bone. This may also account for a lack of microbial activity compared to the relative alkalinity of the other caves. As per Reed's observation (2009) high organic input with available sugar and proteins is readily utilised. A large input can provide a refuge within stable microenvironments created by successional behaviour and heat conduction from metabolic activity of microbes, visibly fungi. Biofilms and fungal blankets create microenvironments by maintaining heat and provide protection against UV radiation (Janaway et al. 2009, Keenan and Engel 2017, Molina et al. 2019).

The presence of phototrophic organisms is evident in open caves and twilight zones of BL-5U4,5,6, LO-5U34 and SP-5U35. However, sunlight is the only motivation for phototrophic damage (Hospitaleche et al. 2011), which can be extensive once the organism is established. The lack of light disabled the cyanobacteria from growing on the CR-5U56 bone (Hospitaleche et al. 2011).

The high dissimilarity between fungi in caves and cave zones reflects the effectivity of air dispersal, through the different cave entrances; low diversity within the walk-in entrance and far rear chamber of CR-5U56, the descending diversity from BL-5U4,5,6 entrance, the high diversity around entrances in VFC-5U1 and highest diversity within the open pitfall entrance of LO-5U34. There is only a fungal profile within dung to assess for SP-5U35, likewise, this indicates a unique fungal diversity and would benefit further microbial profiling within the cave.

In spite of the oligotrophic conditions within the rear chamber of CR-5U56, highly adapted and adaptable fungi persist on low nutrient substrates regardless of metabolic origins. Despite perceivable metabolic preference for higher temperatures and highly nutritious substrates, such as the dung, metabolic adaptivity enables persistence. The occurrence of fungal species within the front of CR-5U56 cave and rear indicate dispersal into the cave and corresponding with an intentional use of pesticide most likely originated from insect activity during kangaroo decomposition.

The introduction of fungi diversity from insects seen in CR-5U56, BL-5U4,5,6 and VF-5U1 indicates dispersal is driven by airflow, insects and animals. Fungi can persist in oligotrophic environments providing environmental humidity and stability, regardless of metabolic origins. Temperatures for metabolic activity may be optimum closer to the entrance; however, cooler temperatures only seem to slow microbial activity but not stop it. High nutrient inputs provoke rapid growth of microbes, and provide a microenvironment contra to the macroenvironment, enabling effective decomposition of highly nutrient substrates. Phototrophic bacteria appear to threaten structural integrity of bones within photic zones; although open environments may slow metabolic activity that prevents noticeable MFD. Fungi has a high degradative influence on bones over relatively short time scales, irrespective of metabolic preference for organic materials over inorganic.

Limited sunlight, high nutrients, bacterial activity and hydrology may result in early permineralisation and survivability of bones in the photic zone of SP-5U35; however, this requires deeper analyses.

Open caves with dynamic environments are more conducive to higher diversities, however, diversity does not appear to threaten bone substrates when metabolic activity is reduced by environmental desiccation. This desiccation may enhance long term survival of bone, in the absence of phototrophic bacteria.

Distant chambers and closed caves provide less diverse communities and limit phototrophic activity, however those that persist are either niche species or metabolically adaptable within oligotrophic environments. Extremophiles may persist in soil and cause eventual degradation of bone; however, fungi appear to rapidly colonise and destroy bone structures before this may occur.

6. CONCLUSIONS

Caves are highly individual in their interactions with outside environments resulting from the entrance structure. These interactions are reflected by the mediated microbial communities within the caves. Diversity of microbial communities appear unique not only between caves from air currents, organic material, soil, hydrology, and visitors; but, between cave zones by airflow/convection, animal and passive transport from visitors with insects proving to be high dispersers of fungi.

Moreover, diversity is not conducive to bioerosion on bones. The open caves displayed higher levels of diversity although environmental parameters restrict metabolic activity of many that are not niche adapted. The environmental parameters encouraging destructive metabolisms appear to be humidity, sunlight, and nutritional input. Although all these environmental effects are moderated by the entrance structure. Therefore, it

becomes apparent that closed caves , regardless of oligotrophy, provide humidity and stability for highly adaptable microorganisms, such as fungi. This may suggest detrimental consequences for exposed fossil beds with increasing nutrition and accessibility to novel metabolisms of fungal species.

Vertebrate fossil provide historical data from which the history of life and environments on Earth may be reconstructed. They are a primary method for studying environmental changes and evolutionary patterns and processes. In order to reconstruct these histories tourist caves displaying fossil beds provide imperative knowledge and in order to prevent destruction of these resources a better understanding of environmental and anthropogenic influences require analyses.

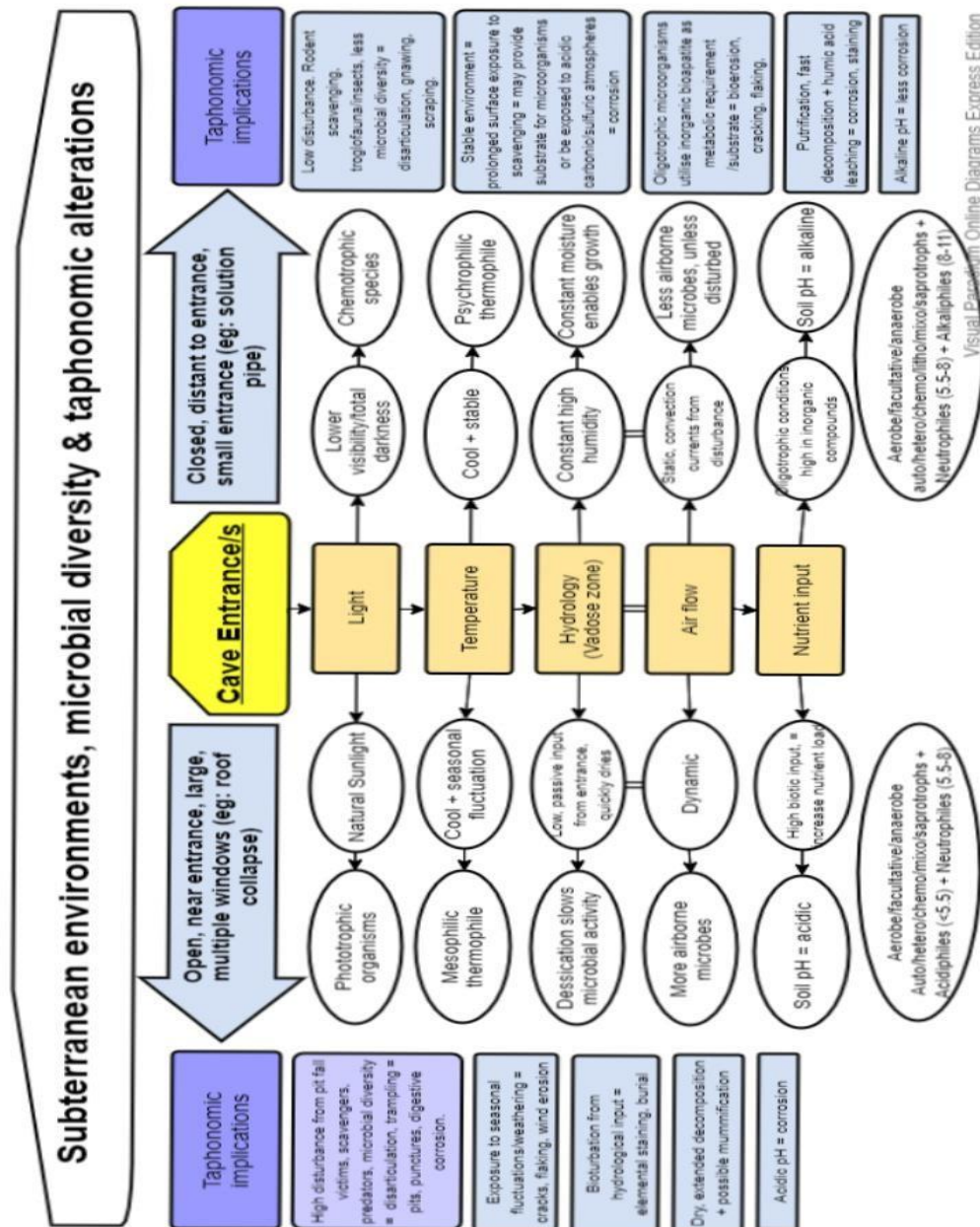


Figure 17: A conceptual flow diagram for observations and conclusions made within this study. Diagram details cave types, environments, factors affecting environments, the microbes associated and the effect on the fossil bone.

7. FUTURE PROSPECTS:

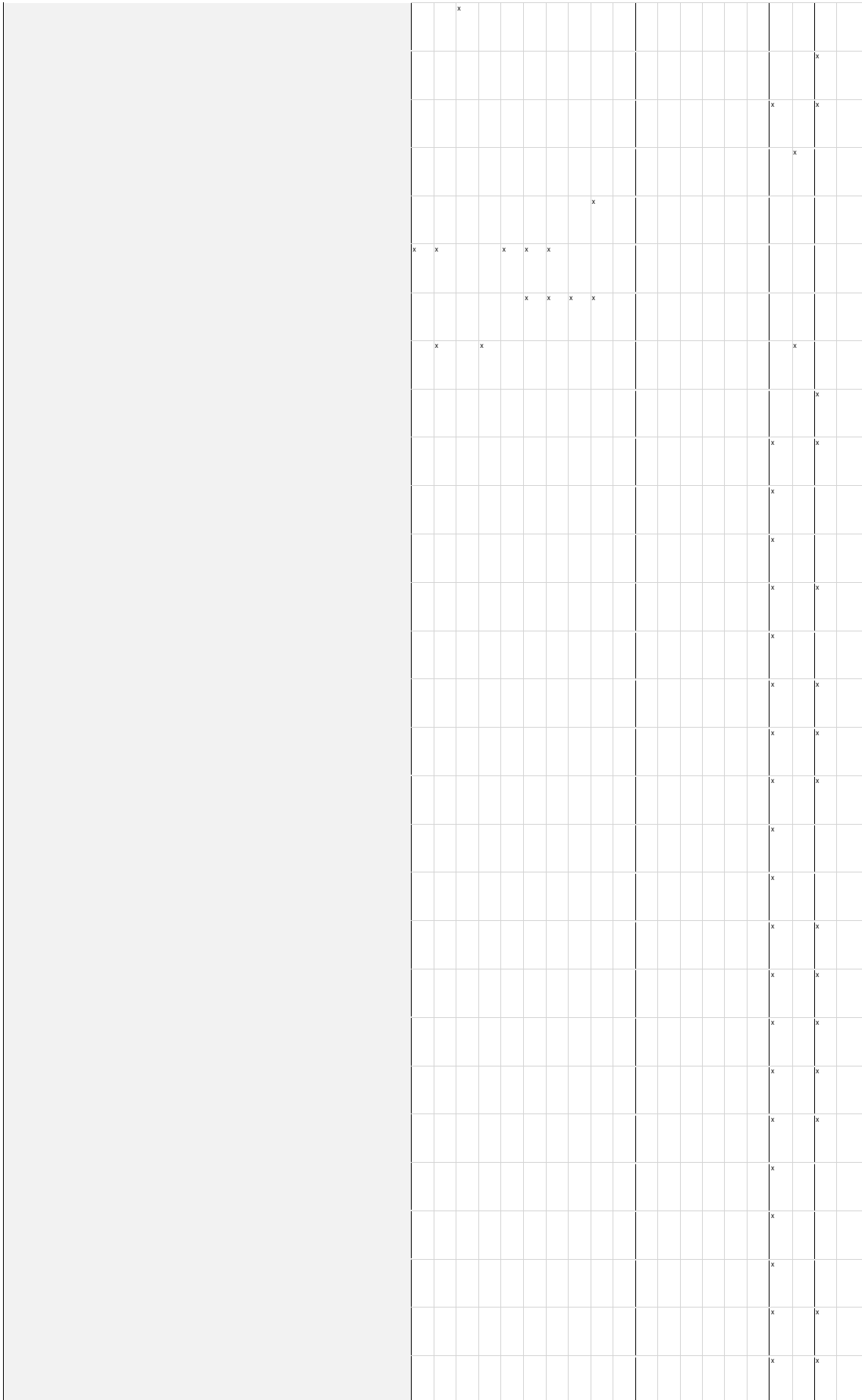
- EDS spectral analysis of bone combined with elemental analysis of soil to contrast elemental changes created by environment and microbe. this will help to elucidate diagenetic stage of organic and inorganic bone diagenesis and mineralogy changes from bioerosion.
- Microbial assessment of the entrance zone and environment within SP-5U35 combined with EDS for preservation analyses of bones.
- Metabolic assessment of chitinophagus and keratophilic fungi on bone in oligotrophic cave conditions and the implications of using biocontrol around karst environments.
- Fungal profiling on insects and dispersal patterns within and between subterranean environments

8. ACKNOWLEDGMENTS

I would like to acknowledge my supervisor Liz Reed for her imperative knowledge, feedback, patience and for enabling this great opportunity. To Steve Bourne for his caving expertise, assistance in getting me out of tight spots and for the photographs. John Conran, for his invaluable input on data analysis. to Virginie and Vicki for advice with last minute laboratory requirements and use of materials. I would also like to thank Benjamin at Adelaide Microscopy and Alex for their assistance with histological preparation of bone for imaging. Importantly, thank you to the private landowners of Crawford's Dead Sheep Cave and Specimen Cave and to Naracoorte Caves National Park for allowing me to conduct research in your inspiring caves. I would like to acknowledge the Australian Genome Research Foundation. A sincere thank you to Pam Catcheside for her priceless knowledge on fungi. Moreover, a heartfelt thank you to Jill

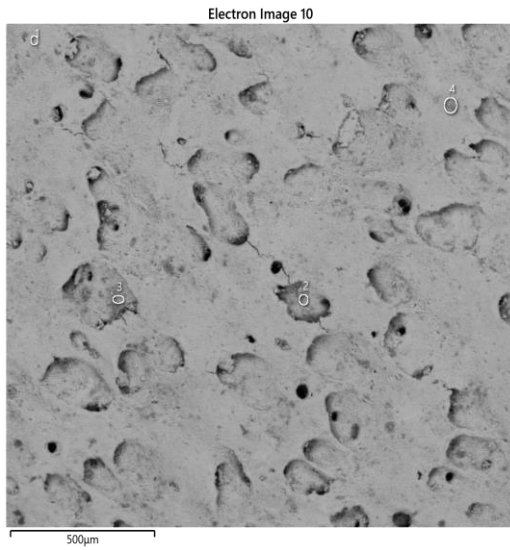
The table consists of a grid with 20 columns and 25 rows. The first column is shaded grey. The remaining 19 columns contain 'x' marks in various patterns. The 'x' marks are distributed as follows:

Row	Col 2	Col 3	Col 4	Col 5	Col 6	Col 7	Col 8	Col 9	Col 10	Col 11	Col 12	Col 13	Col 14	Col 15	Col 16	Col 17	Col 18	Col 19
1																		
2																		
3																		
4																		
5																		
6																		
7																		
8																		
9																		
10																		
11																		
12																		
13																		
14																		
15																		
16																		
17																		
18																		
19																		
20																		
21																		
22																		
23																		
24																		
25																		



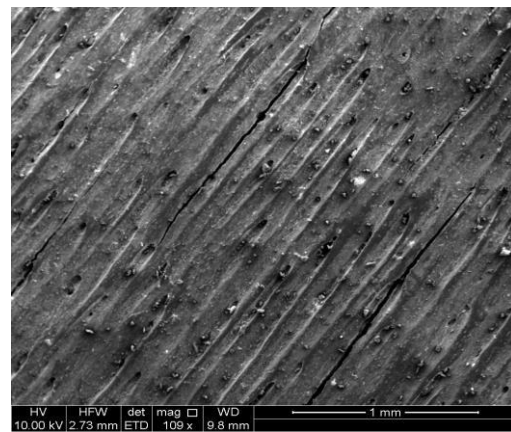
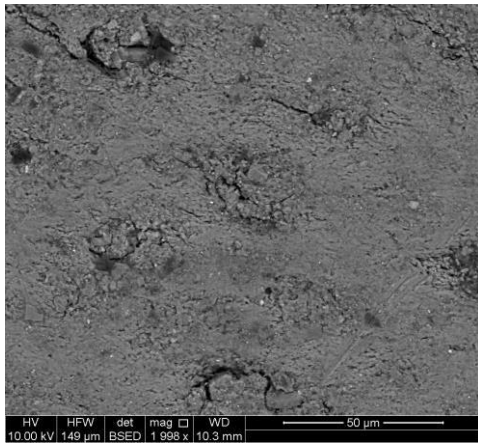
Brooke Emily Lorincz Bioerosion of bones in caves at Naracoorte

NARACOORTE CAVES FUNGAL DIVERSITY PROFILE																										
Cave	SU1 Victoria fossil										SU4, 5, 6 Blanche					SU3 Lost		SU4 Overlook								
	Atmospheric										Atmospheric					Soil	Bone	Soil	Bone							
	Closed, 2 vertical entrance doors										Open, 3 roof collapse windows					Open, roof collapse	Open, roof collapse	Open, roof collapse	Open, roof collapse							
Sample type	~ 90% humidity, 16-19°C										~50-75% humidity (seasonal), 6-15°C					*80-110% humidity, 6-15°C	Open, roof collapse	Open, roof collapse	Open, roof collapse	Open, roof collapse						
Entrance type	Dark, Artificial lights only										Natural/ low light/ Artificial light					Twilight	Dark	Dark	Dark							
Humidity & temperature	Dark, Artificial lights only										Natural/ low light/ Artificial light					Twilight	Dark	Dark	Dark							
Light	Dark, Artificial lights only										Natural/ low light/ Artificial light					Twilight	Dark	Dark	Dark							
High disturbance vs Low disturbance	LD	HD	HD	HD	LD	LD	LD	LD	LD	LD	LD	LD	LD	LD	LD	LD	LD	LD	LD	LD	LD	LD	LD	LD		
Location	V1-5	V1-10	V1-4	V1-3	V1-8	V1-7	V1-2	V1-9	V1-6	BL-2	BL-5	BL-6	BL-3	BL-1	BL-4	LO-1	LO-2	CR-1	CR-2	LD	LD	LD	LD	LD	LD	
Taxon	ENT	AEG	HW	BVA	BLK	GH	FLSBD	ALN	CHX	CHT	ENT	STAG	STOR	MID	DIG	SKL	3m from entrance	50m from entrance								
No blast hit, Other																										
Other																										
Other																										
Other																										
Other																										
Other																										
Other																										
Other																										
Other																										
Other																										
Other																										
Other																										
Other																										
Other																										
Other																										
Other																										
Other																										
Other																										
Other																										
Other																										
Other																										
Other																										
Other																										
Other																										
Other																										
Other																										
Other																										
Other																										
Other																										
Other																										
Other																										
Other																										
Other																										
Other																										
Other																										
Other																										
Other																										
Other																										
Other																										
Other																										
Other																										
Other																										
Other																										
Other																										
Other																										
Other																										
Other																										
Other																										
Other																										
Other																										
Other																										
Other																										
Other																										
Other																										
Other																										
Other																										
Other																										
Other																										
Other																										
Other																										
Other																										
Other																										
Other																										
Other																										
Other																										
Other																										
Other																										
Other																										
Other																										
Other																										
Other																										
Other																										
Other																										
Other																										
Other																										
Other																										
Other																										
Other																										
Other																										
Other																										
Other																										
Other																										
Other																										
Other																										
Other																										
Other																										
Other																										
Other																										
Other																										



CR-5U56 Tibia surface

CR-5U56 Tibia surface



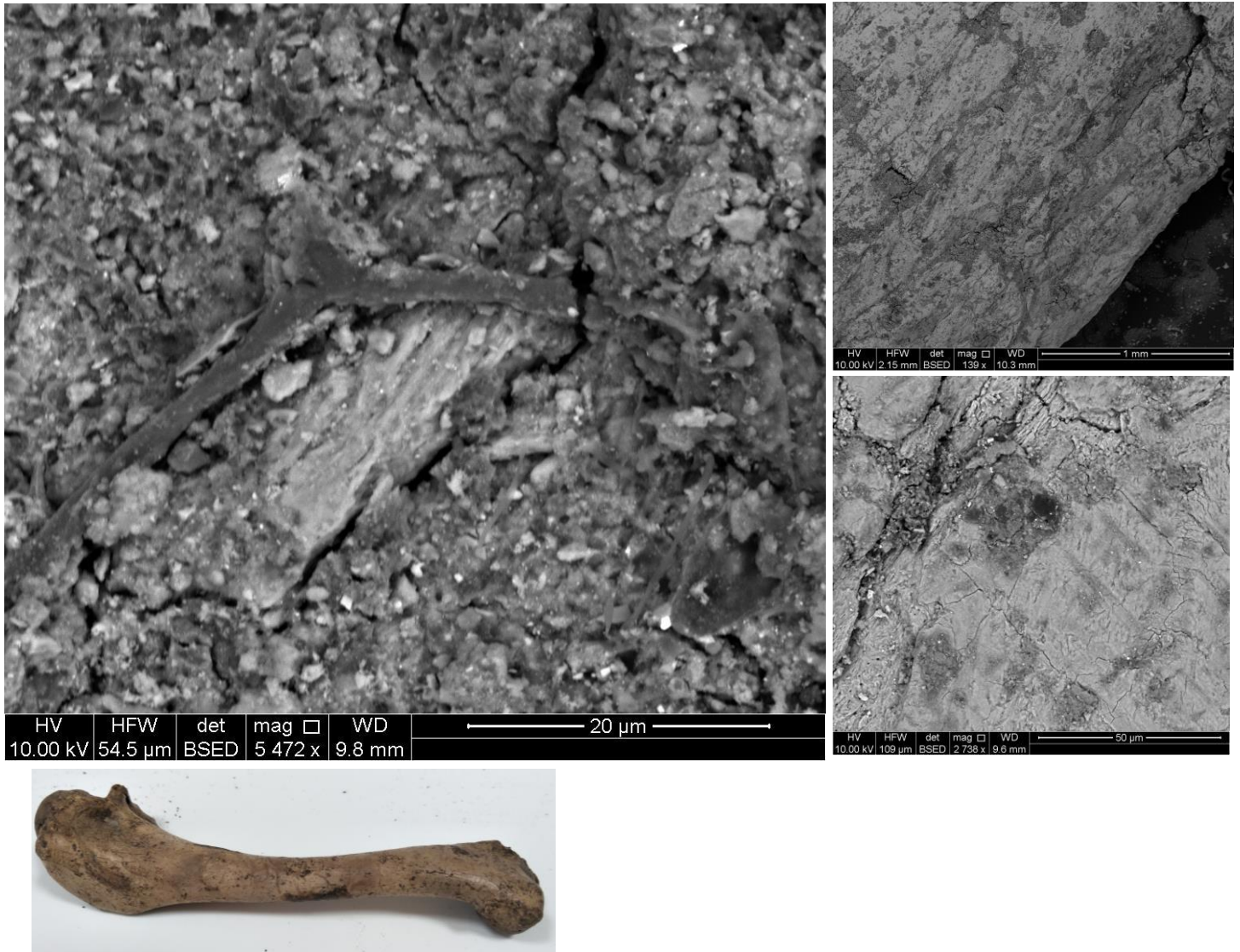


Image: A) 5U35 humerus from sediment cone displays striations radiating from focal site of destruction mid-diaphysis. B) SEM BSE of destruction. Actinobacterial hypha with apical swelling. Fungal hypha. Mucilage of bacteria. C) SEM BSE. Black arrows indicate striations infilled with sediment D) EDS

REFERENCES

- ADETUTU E., *et al.* 2012 Bacterial community survey of sediments at Naracoorte Caves, Australia, *International Journal of Speleology*, vol. 41, no. 2, pp. 137-147.
- ADETUTU E. M., *et al.* 2011 Phylogenetic diversity of fungal communities in areas accessible and not accessible to tourists in Naracoorte Caves, *Mycologia*, vol. 103, no. 5, pp. 959-968.
- BEHRENSMEYER A. K. 1978 Taphonomic and Ecologic Information from Bone Weathering, *Paleobiology*, vol. 4, no. 2, pp. 150-162.
- BOURMAN R. P., MURRAY-WALLACE C. V. & HARVEY N. 2016 The Coorong Coastal Plain and the Limestone Coast. South Australia: University of Adelaide Press, South Australia.
- BREHM U., GORBUSHINA A. & MOTTERSHEAD D. 2005 The role of microorganisms and biofilms in the breakdown and dissolution of quartz and glass,

- Palaeogeography, Palaeoclimatology, Palaeoecology*, vol. 219, no. 1-2, pp. 117-129.
- CHIMUTSA M., *et al.* 2015 Soil fungal community shift evaluation as a potential cadaver decomposition indicator, *Forensic Science International*, vol. 257, pp. 155-159.
- DANIEL J. C. & CHIN K. 2010 THE ROLE OF BACTERIALLY MEDIATED PRECIPITATION IN THE PERMINERALIZATION OF BONE, *Palaios*, vol. 25, no. 8, pp. 507-516.
- FERNANDEZ-CORTES A., *et al.* 2011 Detection of human-induced environmental disturbances in a show cave, *Environmental science and pollution research international*, vol. 18, no. 6, p. 1037.
- FERNANDEZ-JALVO Y. 2016 Atlas of Taphonomic Identifications 1001+ Images of Fossil and Recent Mammal Bone Modification. (1st ed. 2016. edition). Springer Netherlands, Dordrecht.
- FERNÁNDEZ-JALVO Y., *et al.* 2010 Early bone diagenesis in temperate environments: Part I: Surface features and histology, *Palaeogeography, Palaeoclimatology, Palaeoecology*, vol. 288, no. 1, pp. 62-81.
- GADD G. M. 2011 Geomycology. In REITNER J. & THIEL V. eds. Encyclopedia of Geobiology. pp. 416-432. Dordrecht: Springer Netherlands.
- GOLUBIC S., PERKINS R. & LUKAS K. 1975 Boring Microorganisms and Microborings in Carbonate Substrates. pp. 229-259.
- GÓMEZ-CORNELIO S., *et al.* 2012 Succession of fungi colonizing porous and compact limestone exposed to subtropical environments, *Fungal Biology*, vol. 116, no. 10, pp. 1064-1072.
- HACKETT C. J. 1981 Microscopical Focal Destruction (Tunnels) in Exhumed Human Bones, *Medicine, Science and the Law*, vol. 21, no. 4, pp. 243-265.
- HARKE H. 2000 The archaeology of death and burial, *Mortality*, vol. 5, no. 3, p. 325.
- HOSPITALECHE C., *et al.* 2011 Lichen Bioerosion on Fossil Vertebrates from the Cenozoic of Patagonia and Antarctica, *Ichnos*, vol. 18, no. 1.
- JANAWAY R. C., PERCIVAL S. L. & WILSON A. S. 2009 Decomposition of Human Remains. In PERCIVAL S. L. ed. Microbiology and Aging: Clinical Manifestations. pp. 313-334. Totowa, NJ: Humana Press.
- JANS M. M. E. 2008 Microbial bioerosion of bone – a review. Berlin, Heidelberg: Springer Berlin Heidelberg, Berlin, Heidelberg.
- JANS M. M. E., *et al.* 2004 Characterisation of microbial attack on archaeological bone, *Journal of Archaeological Science*, vol. 31, no. 1, pp. 87-95.
- JIANG J.-R., CAI L. & LIU F. 2017 Oligotrophic fungi from a carbonate cave, with three new species of *Cephalotrichum*, *Mycology*, vol. 8, no. 3, pp. 164-177.
- KASEM M. A., RUSSO R. E. & HARITH M. A. 2011 Influence of biological degradation and environmental effects on the interpretation of archeological bone samples with laser-induced breakdown spectroscopy, *J. Anal. At. Spectrom.*, vol. 26, no. 9, pp. 1733-1739.
- KAWATANI M., *et al.* 2008 identification of an osteoclastogenesis inhibitor through the inhibition of glyoxalase I, *Proceedings of the National Academy of Sciences of the United States of America*, vol. 105, no. 33, pp. 11691-11696.
- KEENAN S. W. & ENGEL A. S. 2017 Early diagenesis and recrystallization of bone, *Geochimica et Cosmochimica Acta*, vol. 196, p. 209.
- KENDALL C., *et al.* 2018 Diagenesis of archaeological bone and tooth, *Palaeogeography, Palaeoclimatology, Palaeoecology*, vol. 491, pp. 21-37.

- LANGENFELD A., *et al.* 2011 Insecticidal cyclodepsipeptides from *Beauveria felina*, *Journal of natural products*, vol. 74, no. 4, p. 825.
- MACKEN A. C., *et al.* 2011 Application of sedimentary and chronological analyses to refine the depositional context of a Late Pleistocene vertebrate deposit, Naracoorte, South Australia, *Quaternary Science Reviews*, vol. 30, no. 19-20, pp. 2690-2702.
- MARCHIAFAVA V., BONUCCI E. & ASCENZI A. 1974 Fungal osteoclasia: a model of dead bone resorption, *Calcified Tissue Research*, vol. 14, no. 1, pp. 195-210.
- MAURER A.-F., *et al.* 2014 Bone diagenesis in arid environments: An intra-skeletal approach, *Palaeogeography, Palaeoclimatology, Palaeoecology*, vol. 416, pp. 17-29.
- METCALF J. L., *et al.* 2016 Microbial community assembly and metabolic function during mammalian corpse decomposition, *Science*, vol. 351, no. 6269, p. 158.
- MIYAZAKI T., *et al.* 2011 Evaluation of osteoclastic resorption activity using calcium phosphate coating combined with labeled polyanion, *Analytical Biochemistry*, vol. 410, no. 1, pp. 7-12.
- MOLINA C., *et al.* 2019 Identification of Bacterial and Fungal Species in Human Cadavers Used in Anatomy Teaching/Identificación de Especies Bacterianas y Fungicas en Cadáveres Humanos Utilizados en la Enseñanza de la Anatomía, *International Journal of Morphology*, vol. 37, no. 2, p. 473.
- OGÓREK R., VISOVSKÁ Z. & TANCINOVÁ D. 2016 Mycobiota of Underground Habitats: Case Study of Harmanecká Cave in Slovakia, *Microbial Ecology*, vol. 71, no. 1, pp. 87-99.
- OWOCKI K., *et al.* 2016 Fungal Ferromanganese Mineralisation in Cretaceous Dinosaur Bones from the Gobi Desert, Mongolia, *PLOS ONE*, vol. 11, no. 2, p. e0146293.
- PACZKOWSKI S. & SCHÜTZ S. 2011 Post-mortem volatiles of vertebrate tissue, *Applied Microbiology and Biotechnology*, vol. 91, no. 4, pp. 917-935.
- PACZKOWSKI S., SCHÜTZ S. J. A. M. & BIOTECHNOLOGY 2011 Post-mortem volatiles of vertebrate tissue, vol. 91, no. 4, pp. 917-935.
- PESQUERO M. & FERNANDEZ-JALVO Y. 2014 Bioapatite to calcite, an unusual transformation seen in fossil bones affected by aquatic bioerosion, *Lethaia*, vol. 47, no. 4, pp. 533-546.
- POPOVIC S., *et al.* 2015 Cyanobacteria, algae and microfungi present in biofilm from Bozana Cave (Serbia), *International Journal of Speleology*, vol. 44, no. 2, pp. 141-141.
- PRITSCH K. & GARBAYE J. 2011 Enzyme secretion by ECM fungi and exploitation of mineral nutrients from soil organic matter, *Official journal of the Institut National de la Recherche Agronomique (INRA)*, vol. 68, no. 1, pp. 25-32.
- REED E. 2009 Decomposition and Disarticulation of Kangaroo Carcasses in Caves at Naracoorte, South Australia, *Journal of Taphonomy*, vol. 7, pp. 265-284.
- 2012 OF MICE and MEGAFUNA: NEW INSIGHTS into NARACOORTE'S FOSSIL DEPOSITS, *Journal of the Australasian Cave and Karst Management Association*, vol. 86, pp. 7-14.
- REED E. & BOURNE S. 2000 PLEISTOCENE FOSSIL VERTEBRATE SITES OF THE SOUTH-EAST REGION OF SOUTH AUSTRALIA, *Transactions of the Royal Society of South Australia, Incorporated: incorporating the records of the South Australian Museum*, vol. 124, pp. 61-90.
- RITZ K. & YOUNG I. M. 2004 Interactions between soil structure and fungi, *Mycologist*, vol. 18, no. 2, pp. 52-59.

- STUART E. J. & JAY T. L. 2010 Dormancy contributes to the maintenance of microbial diversity, *Proceedings of the National Academy of Sciences*, vol. 107, no. 13, p. 5881.
- TIBBETT M. & CARTER D. 2009 Research in Forensic Taphonomy: A Soil-Based Perspective. pp. 317-331.
- TRUEMAN C. N. & MARTILL D. M. 2002 The long-term survival of bone: the role of bioerosion, *Archaeometry*, vol. 44, no. 3, pp. 371-382.
- TURNER-WALKER G. 2019 Light at the end of the tunnels? The origins of microbial bioerosion in mineralised collagen, *Palaeogeography, Palaeoclimatology, Palaeoecology*, vol. 529, pp. 24-38.
- VANDERWOLF K., *et al.* 2013 A world review of fungi, yeasts, and slime molds in caves, *International Journal of Speleology*, vol. 42, no. 1, pp. 77-96.
- WEDL C. 1865 Über einen im Zahnbeim und Knochen keimenden Pilz, *Sitzungsberichte der Kaiserlichen Akademie der Wissenschaften. MathematischNaturwissenschaftliche Classe.*, vol. 50, pp. 171-193.
- WHITE S. & WEBB J. A. 2015 The influence of tectonics on flank margin cave formation on a passive continental margin: Naracoorte, Southeastern Australia, *Geomorphology*, vol. 229, pp. 58-72.
- WISSHAK M. 2012 *Microbioerosion*. Elsevier Science & Technology.
- YUAN Y., *et al.* 2016 The relationship between pH and Bacterial Community in a Single Karst Ecosystem and Its Implication for Soil Acidification, *Frontiers in Microbiology*, vol. 7.
- ZHANG Z. F., *et al.* 2017 Culturable mycobiota from Karst caves in China, with descriptions of 20 new species, *Persoonia*, vol. 39, pp. 1-31.